



INSTITUTE FOR DEFENSE ANALYSES

**Roadmap to Evaluate the Risk of Spinal  
Compression Fracture (SCF) Due to  
Electromuscular Incapacitation (EMI)**

Corinne M. Kramer  
Jeremy A. Teichman  
Yevgeny Macheret

November 2016

Approved for public release;  
distribution is unlimited.

IDA Document D-8268

Log: H 16-001289

INSTITUTE FOR DEFENSE ANALYSES  
4850 Mark Center Drive  
Alexandria, Virginia 22311-1882



*The Institute for Defense Analyses is a non-profit corporation that operates three federally funded research and development centers to provide objective analyses of national security issues, particularly those requiring scientific and technical expertise, and conduct related research on other national challenges.*

#### About This Publication

This work was conducted by the Institute for Defense Analyses (IDA) under contract HQ0034-14-D-0001, Project DU-2-4140, "Spinal Compression Fracture Modeling," for the Joint Nonlethal Weapons Directorate (JNLWD). The views, opinions, and findings should not be construed as representing the official position of either the Department of Defense or the sponsoring organization.

#### For More Information

Corinne M. Kramer, Project Leader  
ckramer@ida.org, 703-578-2805

Leonard J. Buckley, Director, Science and Technology Division  
lbuckley@ida.org, 703-578-2800

#### Copyright Notice

© 2017 Institute for Defense Analyses  
4850 Mark Center Drive, Alexandria, Virginia 22311-1882 • (703) 845-2000.

This material may be reproduced by or for the U.S. Government pursuant to the copyright license under the clause at DFARS 252.227-7013 (a)(16) [Jun 2013].

INSTITUTE FOR DEFENSE ANALYSES

IDA Document D-8268

**Roadmap to Evaluate the Risk of Spinal  
Compression Fracture (SCF) Due to  
Electromuscular Incapacitation (EMI)**

Corinne M. Kramer  
Jeremy A. Teichman  
Yevgeny Macheret



## Executive Summary

---

Electromuscular incapacitation (EMI) devices, such as the TASER<sup>®</sup> family of weapons, use conducted energy to produce strong muscle contractions in the target, causing loss of muscle control and incapacitation. EMI weapons have been employed routinely for over 15 years by law enforcement in the United States and by the U.S. military and are recognized as safe and effective. Although estimates vary, the introduction of EMI weapons in 2000 to law enforcement jurisdictions has greatly reduced the use of deadly force by officers and the rate of injuries suffered by officers (Hopkins and Beary 2003), while experiments performed on surrogates and carefully monitored field experience (Eastman et al. 2008; Angelidis et al. 2009; Bozeman et al. 2009; Home Office 2011) establish that the rate of reported injuries due to use of the weapons is extremely low. As of 2009, the total applications of EMI weapons on humans were over 1.74 million (Brewer and Kroll 2009).

Military requirements to extend the duration and delivery range of an EMI weapon have provoked studies that explore the safety of extended duration usage of the existing waveform and changes to waveform parameters to optimize power usage (and thus size, weight, and power (SWaP)) while maintaining effectiveness. Recent swine testing of a new EMI waveform performed at the Air Force Research Laboratory (AFRL) in 2012 (unpublished) produced spinal compression fracture (SCF) in the test subjects and was subsequently confirmed by another AFRL experiment in 2015 (Burns et al. 2015). With a dorsal application of the new EMI stimulus, 43% of all subjects experienced a fracture (confirmed by necropsy). Such reports had never been documented in swine (even under similar conditions and waveform parameters, although probe placement varies). Such fractures in humans as a result of EMI use have been reported only twice in the literature (Winslow et al. 2007; Sloane, Chan, and Vilke 2008). The lack of such reports in humans establishes as negligible the risk of significant injury (RSI) of SCF in the human population using currently fielded weapons. Overall risk of fracture injuries (to include those caused by falls) has been estimated at less than 0.5% (Kenny et al. 2012).

As efforts go forward to improve the EMI weapon for military use, changes may be made to the waveform, and these changes could alter the acceptable rate of SCF to humans. Given the inability to conduct human testing of new waveforms, the risk cannot be directly tested. The purpose of this document is to develop a roadmap for the evaluation of risk of significant SCF to humans in light of the new information provided by the AFRL experiment.

Through our analysis, we have concluded that swine are *not* an appropriate surrogate for estimating human skeletal injury rates from EMI use because of the major differences between the function and size of human and swine back musculature and vertebral strengths (pigs have a larger volume of muscles and weaker compressive vertebral strengths due to their quadruped posture). Therefore, we turned to the biomedical literature to evaluate the need to pursue further analysis or experimentation to estimate the likelihood of SCF in humans. We found sufficient physiological basis in the medical literature to support the hypothesis that contraction forces produced by human back muscles can be sufficient to fracture vertebra under EMI conditions and that minor (asymptomatic) fractures may be more common than known. If such fractures are found to be likely, an analysis of significance of the injury must be performed to determine an overall RSI.

In addition, from the literature on EMI experiments in swine and therapeutic electrical stimulation in humans, we found evidence that muscle contraction intensity varies as a function of probe location, wave-shape, pulse repetition rate, pulse charge, and duration. The extent to which contraction strength will increase as a composite function of those parameters is not clear from existing data and must be explored experimentally to evaluate whether either the likelihood or the severity of SCF will be increased or if a combination of parameters is likely to maintain effectiveness and meet the new requirements without increasing the RSI due to SCF. The specific combination of parameters used in the AFRL testing was not found in any documented research on pigs or humans in the literature. Based on our understanding of the dependence of muscle contraction on the previously mentioned factors, we believe that the stimulus may have been stronger than the previously tested waveforms and that the accepted relationship between muscle contraction force and the various waveform parameters (based on leg-pull forces) may not apply to the local stimulus area. Thus, applying an increased magnitude of stimulus directly to the pig's back may have resulted in larger contractile intensities than expected.

We conclude that while the AFRL results are not able to be translated to human risk estimates, there are grounds to pursue further analysis of this risk to humans. We developed a generalized surrogate framework and exercised it for RSI to identify an optimal mix of experimental and computational methods for evaluation of the problem. The roadmap that we propose includes using existing finite element models of the human back muscles and spine to determine muscle contraction intensity and patterns that are likely to cause SCF and experimentation in swine to explore the time-dependent pattern of local muscle contraction as a function of duration, pulse repetition rate, and current. We believe that swine represent an appropriate surrogate of the muscle contraction trends as a function of those parameters and that results can be translated to humans at that level of the surrogate framework. In this way, we conclude that the estimates of RSI will be rigorously determined and that sufficient information will be acquired to evaluate future waveforms.

# Contents

---

1.	Introduction .....	1-1
2.	Background.....	2-1
	A. AFRL Report.....	2-1
	B. Electromuscular Incapacitation: Mechanism and Testing.....	2-2
	C. Factors That May Affect the Strength and Pattern of Muscle Contraction.....	2-5
	1. Location of Probes.....	2-5
	2. Wave Shape.....	2-7
	3. Pulse Repetition Rate .....	2-8
	4. Total Pulse Charge .....	2-10
	5. Duration.....	2-13
	D. Discussion .....	2-13
3.	Vertebral Loading and Injury .....	3-1
	A. Human Spine and Back Musculature .....	3-1
	B. Spinal Loading through Everyday Activities .....	3-4
	1. Measurement and Prediction of Loading .....	3-4
	2. Measured Vertebral Compressive Strength.....	3-6
	3. Discussion .....	3-7
	C. Epilepsy, Tetany, Shock Therapy, and EMI .....	3-8
4.	Surrogate Framework for EMI-Induced Spinal Compression Fractures.....	4-1
	A. Generalized Surrogate Framework.....	4-1
	B. EMI-Induced Spinal Compression Fracture.....	4-4
	C. Transfer Function for Electro-Muscular Porcine to Human Spinal Compression Surrogate .....	4-5
5.	Conclusions and Roadmap .....	5-1
	A. Conclusions .....	5-1
	B. Road Map .....	5-2
	1. Surrogate Experimentation.....	5-2
	2. Human Modeling.....	5-2
	Illustrations .....	A-1
	References.....	B-1
	Abbreviations .....	C-1



# 1. Introduction

---

The Joint Non-Lethal Weapons Directorate (JNLWD) contracted with the Institute for Defense Analyses (IDA) to develop a roadmap for evaluating the risk of spinal compression fracture (SCF) through Electromuscular Incapacitation (EMI) use on humans. The impetus for the study is recent surrogate testing in swine, which resulted in a large percentage (~43%) of spinal compression fractures after a few seconds of EMI application. The experiment was intended to replicate an earlier study where SCF was noted, but not explored in a controlled manner. Further details of this experiment will be discussed in Chapter 2.

Existing EMI weapons operate by discharging electrical stimulus into the target. The electric field stimulates motor and reflex neurons, activating muscle contractions that overwhelm the target's ability to control his/her movement. The weapons, in their currently fielded form, are extremely effective, producing total incapacitation as long as good electrical contact can be made. At the appropriate stimulus rate, muscles are unable to relax between applied pulses and exhibit continuous contractions, a phenomenon known as tetany. These weapons are well liked by law enforcement. Analysis of use of force in multiple jurisdictions confirms that the use of these weapons is associated with reduced rates of injury to suspects and officers (Hopkins and Beary 2003, Jackson, Neeson, and Bleetman 2006). Experiments performed on surrogates as well as carefully monitored field experience (Eastman et al. 2008; Angelidis et al. 2009; Bozeman et al. 2009; Home Office 2011) indicate that the weapons are extremely safe. As of 2009, the total applications of EMI weapons on humans were over 1.74 million (Brewer and Kroll 2009).

The waveform of the electrical stimulus associated with these well-used and reliable weapons has resulted in a diagnosis of SCF in fewer than 10 cases (Burns 2015). Only two cases are published in the open literature (Winslow et al. 2007; Sloane, Chan, and Vilke 2008) out of hundreds of thousands of exposures. Overall risk of fracture injuries (to include those caused by falls) has been estimated at less than 0.5% (Kenny et al. 2012). The rate of spinal compression fracture SCF in swine is unknown since most studies did not focus on this risk and necropsy (i.e., an autopsy) was required to diagnose.

The difference in the experimental sets is significant. We can say conclusively that present waveforms, even when applied directly to the back, do not produce appreciable rates of symptomatic compression fractures in humans. We cannot say the same about swine, since the animals were not revived from anesthesia following the experiments to identify if they were symptomatic. However, we do know that the specific combination of

parameters<sup>1</sup> used in the Air Force Research Laboratory (AFRL) testing was not found in any documented research on pigs or humans. Therefore, the AFRL results do not immediately call into question previous assumptions that such fractures were *not* occurring during EMI testing. Based on our understanding of the dependence of muscle contraction on repetition rate and pulse charge, we believe that the stimulus may have been stronger than the previously tested waveforms and that the local muscle effects may exceed the effects (e.g., leg-pull force) traditionally measured in EMI experiments on swine. Specifically, we have concerns that assumed regions of saturation of muscle contraction forces based on such leg-pull forces remote to the application site may not apply to the local (thoracic) effects.

The new information acquired in the AFRL study (Burns et al. 2015) raises questions about the appropriateness of swine as a surrogate for humans during EMI testing and brings to light a number of unknowns regarding the relationship between EMI waveform parameters and musculoskeletal response and risk of injury in vertebrates.

To address these questions, we developed a generalized framework for surrogate use and exercised it end to end for evaluation of EMI risks to the spine via muscle contraction. We found that for some organ systems, swine are used appropriately as surrogates for humans. For example, the cardiovascular, pulmonary, and lymphatic systems of swine are generally accepted as analogous to human effects (*Pig Manual*, n.d.), and swine show similar biochemical (blood-based) and respiratory characteristics following muscle exertion. Another major benefit of swine as surrogates for humans is that breeds can be selected to approximately match human size, although relative distances (electrode to organs or limbs) will not be well matched (Jauchem et al. 2009). However, an analysis of the anatomy of swine makes clear that they are not an adequate surrogate for human musculoskeletal systems. Pigs are quadrupeds with much higher muscle mass around their spine and lower loading capacity in their vertebrae (Busscher et al. 2010).

The fact that swine are found to be more vulnerable to spinal compression fractures than humans are does not imply that the risks are negligible for humans. It is well known (e.g., from studies of patients that have epilepsy and tetanus and from studies of electroshock therapy patients) that the human back muscles are capable of producing spinal compression fractures. In assessing vertebral loading capacity, we found loads due to lifting weights or other common activities can, in some cases, exceed vertebral compression strength, but unconscious activation of stabilizing muscles reduces the risk of injury. Such control is not available, however, to the EMI target.

---

<sup>1</sup> The AFRL experiment used a dorsal application of a square wave, with 19 or 40 pulses per second (pps), and 60- or 80- $\mu$ C pulse charge for 30 sec.

Given the inadequacy of swine as a surrogate for direct measurement of the risk of spinal compression fracture, the goal of this report is assist the JNLWD in developing a roadmap to explore the risk of SCF to humans from new EMI waveforms, to include modeling and experiment. One option proposed by the AFRL researchers is to perform experiments in primates. Primates represent an improvement over swine in terms of appropriateness as a musculoskeletal surrogate for humans, and these experiments may be conclusive regarding the human risk of SCF due to the specific tested waveform. IDA did not exercise its surrogate framework on primates. However, following costly and logistically challenging primate testing for specific waveforms, the JNLWD would still lack a method of evaluating *new* waveforms for the risk of fracture.

IDA has explored computational modeling options in conjunction with animal testing and has identified existing models at various stages of the EMI process. However, stitching these components together into an end-to-end model of the applied electrical signal to fracture risk represents a significant effort and would not be easy to validate in any case. Instead, IDA proposes using existing validated biomechanical or finite element models of human spine and musculature to explore conditions that may cause SCF and using experimental methods to evaluate the likelihood of specific waveforms that produce those conditions as a function of relevant parameters. For example, what are threshold stresses, over what duration or time pattern do these stresses cause fracture for each vertebrae, and which muscle groups are capable of providing those forces (alone or in combination with other muscle groups)? Also, must several muscle groups be contracting in phase to exceed fracture thresholds, or is it more likely due to asymmetric muscle contraction (could be caused directly by the stimulus or from asymmetric muscle fatigue)?

When the conditions that can cause fracture have been identified, the likelihood of EMI that could result in those conditions may be able to be explored experimentally in humans or an animal surrogate using existing techniques of measuring muscle contraction. Depending on the results of the modeling study, we believe that swine will be an adequate surrogate for this measurement since individual muscle response to electrical signals is similar in all mammals. The translation of muscle activation from swine to human will require a transfer function—a concept that is explained further in Chapter 4.



## 2. Background

---

### A. AFRL Report

**Note:** The term “AFRL report” is used in several places in this document. When used, it refers to the Burns et al. (2015) reference in the Reference List.<sup>2</sup>

Military applications seek solutions for an extended duration and long-range incapacitation effect (Joint Non-Lethal Weapons Directorate 2009). To that end, swine testing has been conducted to estimate the risk of longer duration EMI stimulation and to evaluate alternative waveforms that may require smaller (lighter) battery packs while maintaining the same effectiveness. Testing at the Naval Medical Research Unit (NAMRU) in 2012 unexpectedly produced SCF in the swine test subjects when they were exposed to stimuli at frequencies of 40 Hz, with electrical charges per pulse of 60 and 80  $\mu\text{C}$ .<sup>3</sup> Some of the animals exposed to a 19-Hz stimulus also suffered fracture (Burns, 2015).

A follow-up study conducted at AFRL in 2015 reproduced the test conditions and produced SCF in 43% of anesthetized swine subjects (*Sus scrofa*,<sup>4</sup> n = 40). In some but not all cases, the fracture was audible within 3 sec. of dorsal application of a 40-Hz stimulus and within 20 to 30 sec. of dorsal application of a 19-Hz stimulus. For the 19-Hz stimulation, audible cracks were immediately preceded by a gross motion of the tail-end of the animal into an extreme arched position.

The probes were applied dorsally 5 cm lateral to the spine on the left-side, with a 25-cm separation. The magnitude of muscle contraction was measured using a motion sensor to capture linear and angular acceleration of the limbs. See Figure 2-1.

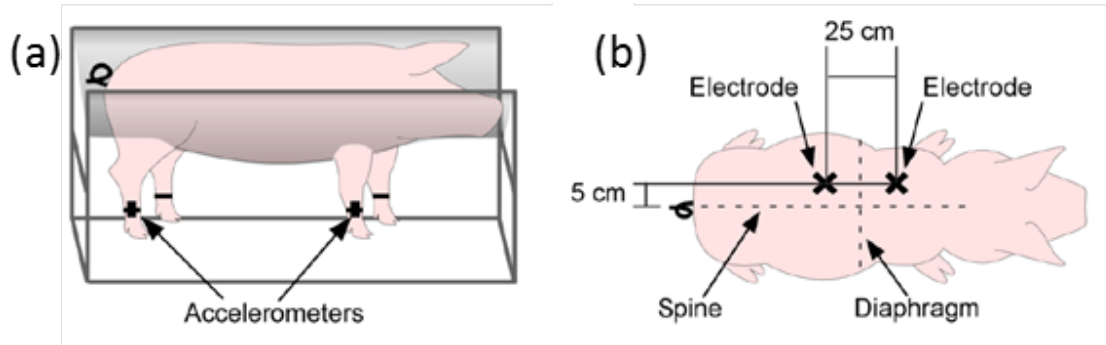
The researchers report that the magnitude of the motor response during stimulation was highly dependent on the repetition rate of the stimulus (19 pulses per second (pps) or 40 pps) but that there was no apparent effect from the magnitude of electric charge per pulse (60  $\mu\text{C}$  or 80  $\mu\text{C}$ ). At both pulse frequencies, three phases of the motor response were identified: (1) whole-body muscle contraction (jerk), (2) tetanic (or continuous) contraction of all the muscles in the body, and (3) muscle relaxation. When stimulated at 19 pps, test

---

<sup>2</sup> Burns, J., M. Kamykowski, J. Moreno, J., and M. Jirjis. 2015. “Prolonged Electromuscular Incapacitation (EMI) in a Porcine Model for Assessment of Spinal Injury.” San Antonio, TX: JBSA Fort Sam Houston, General Dynamics Information Technology.

<sup>3</sup>  $\mu\text{C}$  = microcoulomb.

<sup>4</sup> *Sus scrofa* = Wild boar.



Source: Burns et al. (2015).

Note for Figure 2-1: (a) The pig was placed in a vinyl sling, which allowed the limbs to move freely above the floor during stimulation. The movement of the limbs was captured by the motion sensors; (b) The electrodes were placed on the dorsal surface of the pig such that the electrodes were positioned 5 cm left of the spine and spanned across the diaphragm 25 cm.

**Figure 2-1. Set Up for the AFRL 2015 SCF Experiment**

subjects displayed whole-body convulsions until tetany was achieved (after approximately 15 sec. of stimulation). For a 40-pps stimulus, the test subjects remained relatively still, indicating that tetanus was achieved nearly instantaneously. Muscle relaxation began when the electrical stimulus stopped.

Real-time x-ray fluoroscopy was used to diagnose fracture in the subjects, and dissection was used to confirm. The researchers hypothesize that the higher repetition rate and overall sustained muscle contraction force in the 40-pps data set may have caused fatigue-related stress fractures to occur sooner than they did in the 19-pps data set. We note that the doubled rate of stimulation does not translate simply to a halved onset time, indicating that, if valid, there is a likely dependence on recovery time, which would explain why rate, not number of cycles is a relevant factor.

Overall vertebral fractures in the lumbosacral region were identified in 43% of the test subjects, with approximately equal rates occurring in all data sets (10%: 19 pps, 60  $\mu\text{C}$ ; 10%: 19 pps 80  $\mu\text{C}$ ; 18%: 40 pps, 60  $\mu\text{C}$ ; and 5%: 40 pps, 80  $\mu\text{C}$ ). The fractures were described as extreme (shattering the sacrum and several vertebrae). Such fractures were clearly unstable, indicating they would have been classified as significant if the subjects had been revived.

## **B. EMI: Mechanism and Testing**

An EMI device is designed to stimulate muscle contractions that are strong enough in targets to incapacitate them. The electrophysiology of motor neuron activation and muscle fiber and motor unit contraction is well understood, but experiment is required to establish the most effective parameters on a system level. Generally speaking, individual pulses must deliver sufficient charge over a volume that is large enough to stimulate muscle contraction

in enough muscles to prevent voluntary motion, and the pulses must be repeated sufficiently frequently to prevent relaxation between the pulses. At the other end of the spectrum, individual pulses must not be strong enough to induce major complications, such as ventricular fibrillation, and the pulse repetition rate and duration must not be sufficient enough to induce serious muscle or skeletal damage.

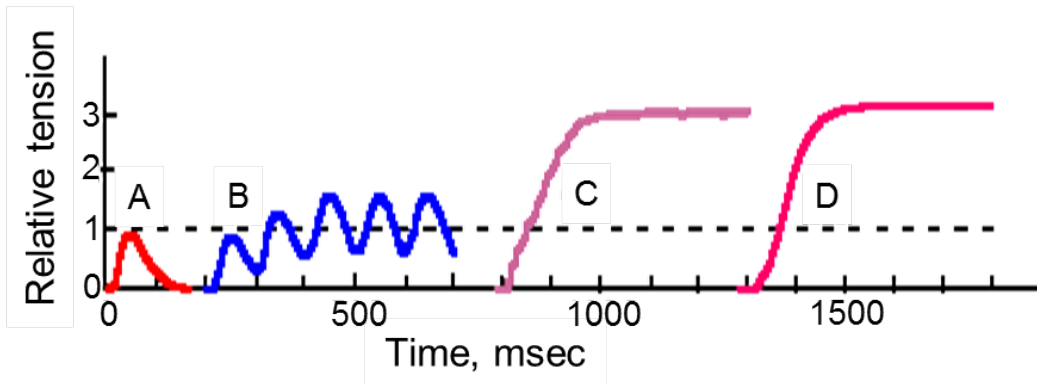
Early waveforms tested by Sherry et al. (2003) operated at lower current and pulse repetition rate than current waveforms and failed to incapacitate the animal (swine) subjects either due to a lack of sufficient muscle recruitment volume or insufficient rate to induce tetany. The animals were reported to run in circles, maintain posture, and even jump during the electrical stimulus. That same year, the TASER X26 was released and offered a sufficient combination of waveform parameters to provide total incapacitation during the duration of stimulus. (IDA did not find any documentation of experimentation supporting this development process.)

A decade and a half of field use and experimentation since then have demonstrated that the TASER<sup>®</sup> waveform is effective and safe. However, advanced weapons may exploit altered waveforms. Here, we review what is known about the EMI effect on muscles based on the medical literature for therapeutic electrical stimulation and EMI weapon testing.

Skeletal muscles are made up of individual fibers, organized in varying geometries and densities into muscle groups and motor units. When a motor neuron is stimulated by an impulse from the brain or an external electrical impulse, an action potential is conducted into the muscle, initiating conformation changes that result in muscle contraction and force generation.

Figure 2-2 shows the time pattern of muscle stimulation due to repeated stimulation for individual pulses (A), repeated pulses (B) repeated pulses at sufficient frequency to induce tetanic contraction (C), and repeated pulses at even higher frequency resulting in fused tetanic contraction (where the contraction is fully continuous, with no evidence that a discrete series of pulses is stimulating) (D).

The shape of the twitch pulse and the necessary rates to develop tetanic and fused tetanic contractions depend on the muscle type. Skeletal muscle fiber can be broken down into slow-twitch (red) and fast-twitch (white) types. Slow-twitch fibers are typically innervated by large axon motor neurons and contract for long periods of time but with lower forces. Fast-twitch muscle fibers are innervated by small axon motor neurons and contract quickly and powerfully but fatigue rapidly. Slow-twitch fibers are reported to have a twitch time of about 75 ms and can develop tetanic fusion (or continuous state of contraction) at 13 to 16 pps. Fast-twitch fibers have a twitch time of about 40 ms and become fused at about 40 to 60 pps (Mann 2016, Chap. 14).



Source: Sherman, Luciano, and Vander (1970).

Note for Figure 2-2: The relative tension of a muscle during repeated stimulation: (A) represents a single-twitch contraction in a fast skeletal muscle; (B) represents the accumulation of tension when muscles are stimulated faster than the relaxation rate (~10 pps); (C) represents unfused tetanus produced by a stimulation rate of ~50 pps; and (D) represents fused tetanus evoked by stimulation at ~100 pps.

**Figure 2-2. Muscle Tension as a Function of Stimulus Rate**

The threshold (E-field) for electrical coupling with a fiber depends on the diameter of the fiber. Direct excitation of muscle fibers from EMI stimulus takes place in between the probes, in the area of greatest electrical field, but motor neurons can excite muscles beyond the region of direct activation and can also be stimulated outside that region due to lower activation thresholds than those of the muscles. Generally speaking, larger fibers require a smaller pulse duration and amplitude to be fired than small fibers do. Direct effects occur along lines of current flow and under electrodes. Indirect effects occur further from the probes and are usually the result of stimulating motor groups innervated by nerves in proximity to the stimulus.

The standard EMI waveform used by TASER Corporation in its commercial products (X26 and M26), including those used by the U.S. military, consists of a pulse train that has pulse widths of 100–155  $\mu\text{s}$ , delivering a charge per pulse of 60–125  $\mu\text{C}$  at a repetition rate of 17 to 19 pps for a duration of 5 sec. Commercial products also include extended duration waveforms, although these products have not been on the market for as long as the X26. For example, the TASER X26C, C2, Pulse, and Bolt have total durations of 30 sec., with decreasing pulse frequency and short breaks between pulse chains. (TASER Corporation Website, n.d.).

The high fracture rate seen in the 2015 AFRL experiment requires a comprehensive analysis of the existing parameter space tested in pigs and in humans. Years of testing in swine and in humans have resulted in a strong knowledge base of effects. Here, we detail as fully as possible the known parameter space and highlight regions that might be exploited to better understand the mechanism and likelihood of such fractures.

## C. Factors That May Affect the Strength and Pattern of Muscle Contraction

We have identified five factors that may affect the strength and pattern of muscle contraction in ways that are relevant to SCF estimates:

- Location of probes,
- Wave shape,
- Pulse repetition rate,
- Total pulse charge, and
- Duration.

We note that pulse duration is an additional factor that may change the effect of an EMI weapon. However, we believe that the TASER<sup>®</sup> is sufficiently constrained at approximately 100  $\mu$ s due to basic design features (activating skeletal as opposed to cardiac muscle); however, we have not explored in the literature for details on the effect of changing pulse width.<sup>5</sup>

### 1. Location of Probes

While the EMI effect encompasses the whole body, the proximity of muscle group to the source is a factor in the magnitude of the muscle response. Specifically, the volume of motor groups captured is highest between the probes (Leitgeb et al. 2010), but stimulation of nerves located between and near the probes activates muscles well outside the area of direct electronic stimulation (e.g., in the limbs) (Reilly and Diamant 2011). To our knowledge, no experiments have captured the geometric relationship of the intensity of muscle contraction to the distance from the probes. In fact, the magnitude of muscle response is exclusively measured as a function of limb movement or force, with application of the probes to the trunk.

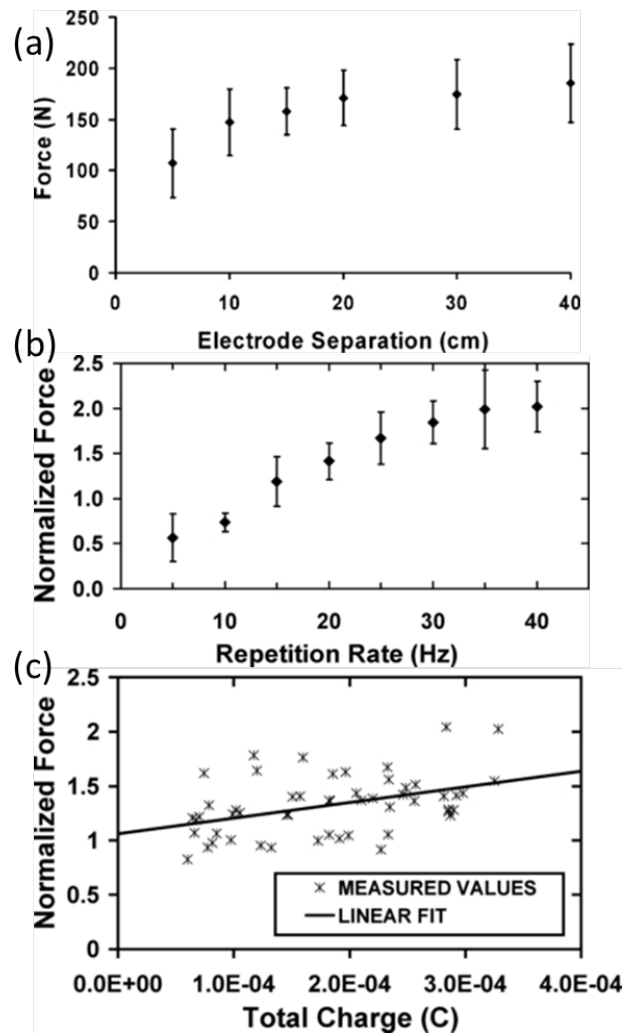
Two aspects potentially relevant to the evaluation of SCF are the proximity to the major muscle groups implicated in compression of the spine and asymmetrical loading. Initial posture, preexisting muscle imbalance, and asymmetry of the response can affect the loading of individual vertebrae and should be explored quantitatively.

In general, probe location is underreported in swine testing. Studies may have applied X26-like doses dorsally, but we found no evidence in the literature. The effect of separation of probes on leg-pull force has been well studied. The magnitude of contraction is observed to plateau at around 20 cm of separation (Beason et al. 2009), as shown in Figure 2-3(a).

---

<sup>5</sup> Note that research is ongoing into a different mechanism of electrical incapacitation based on much shorter (nanosecond to microsecond duration) pulses (Pakhomov et al. 2006). That mechanism is not part of this analysis.

This effect is assumed to be due to increased current density deeper in the body. In addition, for studying the risk of ventricular fibrillation, multiple studies have attempted to model the current flow in the body from EMI stimuli (Leitgeb et al. 2010; Reilly and Diamant 2011). To our knowledge, these models have not been linked to physiological models of muscles to predict contractile state as a function of time and space. However, experiments in animal surrogates could be performed to make such measurements.



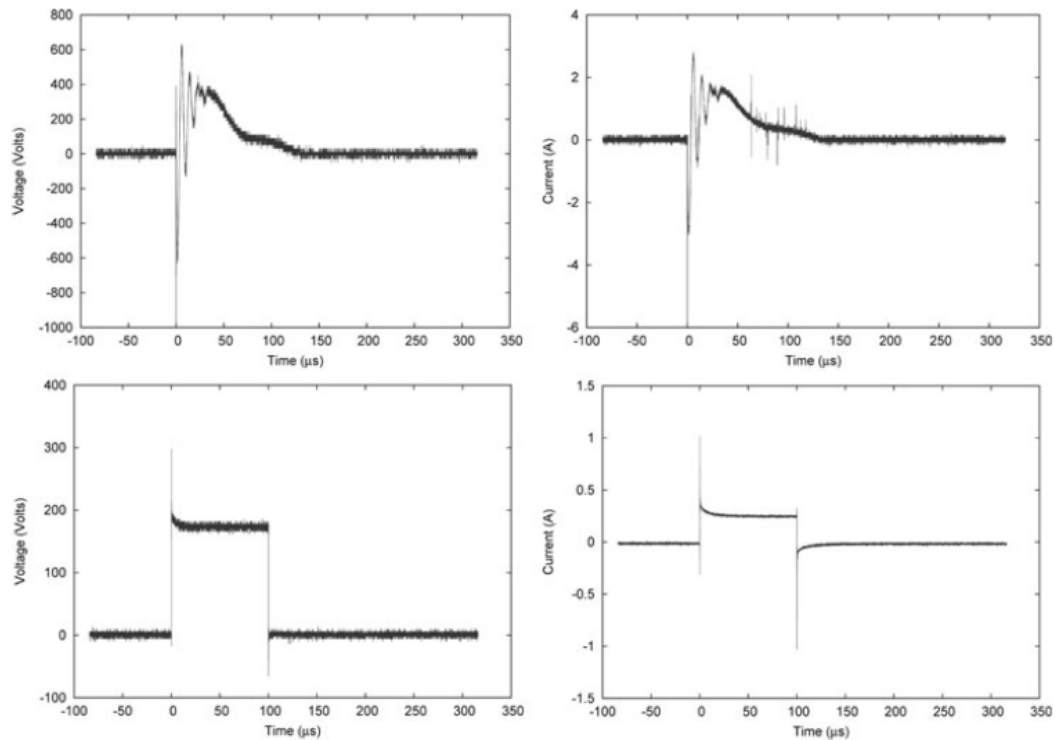
Source: Benson et al. (2009, 1115 (Figures 3, 4, and 5)).

Note for Figure 2-3: The use of a limb to measure net forces does not allow insight into the muscle recruitment patterns but does illustrate that for the given waveform parameters, force begins to plateau with an electrode separation of 20 cm and with a repetition rate of 40 pps. The force as a function of total charge is hypothesized to increase linearly with charge delivered (Beason et al. 2009). Normalized force refers to a comparison between the waveform under study and the traditional TASER X26 waveform.

**Figure 2-3. Dependence of Net Force of a Suspended Swine Limb Attached to a Strain Gauge on EMI Waveform Parameters of Electrode Separation, Pulse Repetition Rate, and Charge Delivered per Pulse**

## 2. Wave Shape

The TASER<sup>®</sup> waveform is a complex pulse with voltage and current from a typical discharge shown in Figure 2-4 (top). Comeaux et al. (2013) explored different waveform shapes (square, Gaussian, increasing exponential, and decreasing exponential) and found that the square pulse required the least energy to provoke the same force response as measured by leg pull in swine. The TASER X26 waveform and a square pulse as used by Comeaux et al. are shown in Figure 2-4.



Source: Comeaux et al. (2013, 1027 (Figure 1)).

Note for Figure 2-4: High-frequency measurement noise can be noticed in the signals shown. This noise was removed with a triangular smoothing algorithm during measurement.

**Figure 2-4 Example Voltage and Current Waveform of a Commercial CEW Pulse (Top) and a Square Pulse from the Laboratory Device (Bottom)**

Comeaux et al. (2013) found that the same effect of the complex TASER<sup>®</sup> waveform could be generated (as measured by leg-pull force in swine experiments) using significantly lower charge per pulse in the square wave but with an increased pulse repetition rate. This discussion continues in the next section, where we introduce the effect of pulse rate and then discuss the combined effects of pulse shape and rate. We are not aware of any physiological reason that the square wave would introduce increases in muscle contraction over the complex TASER<sup>®</sup> waveform and note that most of the effect observed by Comeaux et al. is accounted for by the increased pulse repetition rate. We note, however, that most

historical testing has been conducted with simulated complex waveforms, while the AFRL researchers used a square wave at both 19 and 40 pps.

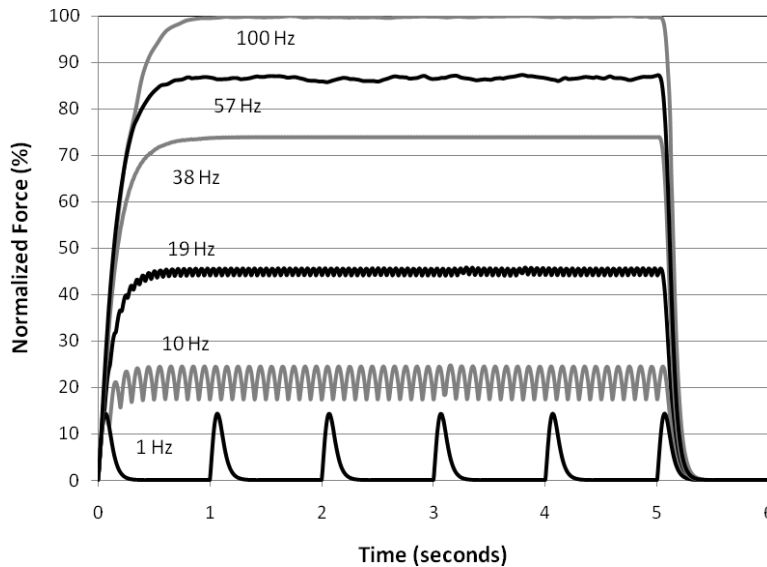
### **3. Pulse Repetition Rate**

The effects of pulse repetition rate on the pattern and intensity of muscle contraction can be understood in terms of the capacity of human muscle to respond to volitional or external stimulus, as discussed in the beginning of this section. Different muscles have different relaxation rates. As new pulses arrive before the muscle has had sufficient time to relax, the contraction becomes continuous (tetany). In addition, the intensity increases as waves of muscle force are superimposed. There is a natural limit to the contractile force that is determined by the muscle shape and size. The magnitude and repetition rate with which to achieve this force are muscle dependent. As the repetition rate is increased beyond that necessary to produce tetany, fused tetany is achieved, at which point individual muscle contractions are indistinguishable and a constant contractile state is observed. Increasing the pulse repetition rate beyond that point should have no effect on muscle contraction. For therapeutic electrical stimulation at low currents, 20–80 pps are generally used (selection of repetition rate depends on the specifics of treatment), and it is generally acknowledged that the magnitude of generated force increases with pulse repetition rate, up until approximately 100 pps (Gad Alon (University of Maryland), pers. comm., 2016).

Beason et al. (2009) explored the relationship between repetition rate and leg-pull force  $i$ , as shown in Figure 2-3(b). The leg force appears to increase by a factor of ~40% between 20 and 40 pps and to plateau between 30 and 40 pps. Comeaux et al. (2013), in their exploration of square wave pulses, observed that fused muscle tetany occurred in swine (via leg pull) at 40 pps (square wave) while unfused tetany was observed at 19 pps with the complex wave shape as shown in Figure 2-4. Using the square wave at 19 and 40 pps, the AFRL researchers observed the same distinction between fused and unfused tetany during leg-pull contractions (Burns et al. 2015).

Sweeney (2009) explored the effects of pulse repetition rate theoretically using a nerve model developed by McIntyre, Richardson, and Grill (MRG) integrated with a skeletal muscle isometric force generation model developed by Ding and colleagues to simulate the forces generated by X26 waveforms. The resultant relationship between forces and pulse repetition rate is shown in Figure 2-5 for frequencies from 1 to 100 Hz (pps).

In Figure 2-6, we plot the maximum relative force normalized to the 19-Hz stimulus in Sweeney's simulation for closer comparison to Beason et al.'s (2009) measurement of leg-pull force as a function of stimulus repetition rate (inset in Figure 2-6 and also normalized to TASER X26 pulses operating at 19 Hz (pps)). The simulated dependence of maximum force levels on pulse repetition rate is consistent with the effect observed in swine



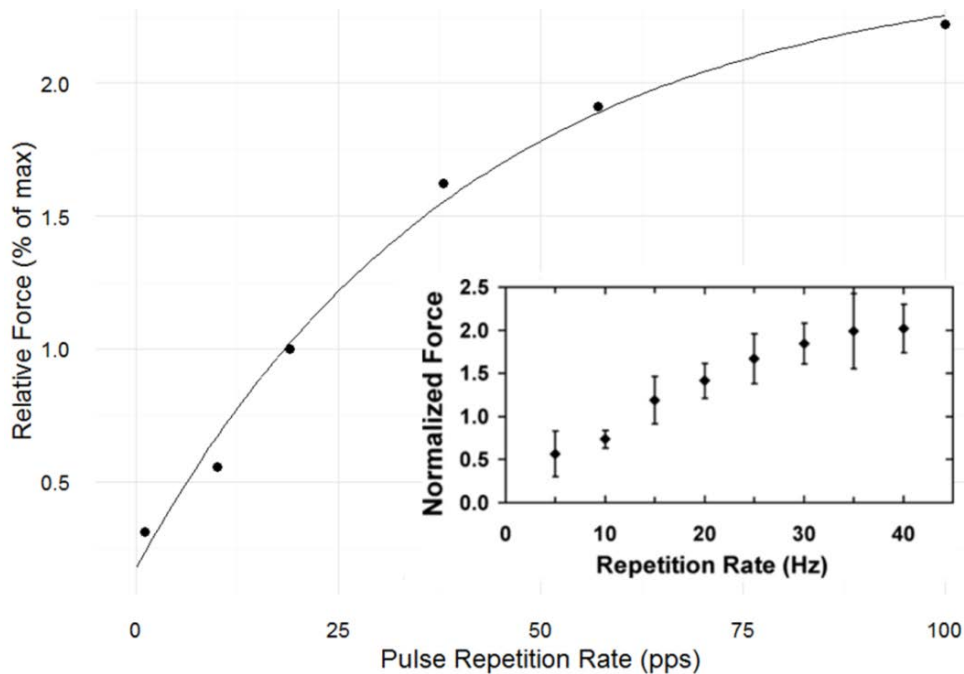
Source: Sweeney (2009, 3190).

Note for Figure 2-5: Individual pulses fuse as the rate is increased from 1 to 10 Hz (pps) and contraction intensity increases as pulses add up. The rate of increase of contraction intensity with pulse repetition rate is observed to decrease as repetition rate increases. Tetany is observed at 10 Hz (pps), and fused tetany is observed between 19 and 38 Hz (pps).

**Figure 2-5. Simulated Contraction Forces as a Function of Stimulus Repetition Rate**

by Beason et al. but with force increasing more steeply (approximately 60% between 19 and 38 Hz (pps) compared to Beason et al.'s 42% and note that the asymptote observed by Beason et al. between 30 and 40 pps is far exceeded in the simulation). The difference between the two forces may be due to simulation or experimental error; however, the data imply that the leg-pull force measurement may not offer adequate insight into the maximum contractile forces in the direct vicinity of the stimulus (as Sweeney (2009) simulated). The leg-pull force may have a diminished dependence on repetition rate since the muscles are remote from the stimulus and represent a net force measurement. Relying on leg-pull force alone may lead to an erroneous conclusion: that contractile forces are saturated as frequency is increased above 30 pps, when forces local to the stimulus may continue to increase.

Although we observe that force may continue to increase with repetition rate above 40 pps, Comeaux et al. (2013) hypothesized that the benefit of higher repetition rate is that the effects of fully fused tetanic contractions may be less traumatic to the muscle and skeletal system. They note that repeated isometric contractions are reported to produce fatigue at shorter time scales than sustained muscle contraction. The effects of fusion may be relevant since stress fractures in vertebrae are often a result of repeated stress (Kelly 1954), not an instantaneous effect based on a single contraction. As noted previously, however, the dependence of the specific muscle groups implicated in spinal compression on pulse repetition rate should be explored, as opposed to the net movement of the limbs.



Source: Modified from Sweeney (2009) (inset Beason et al. (2009)).

Note for Figure 2-6: In this figure, we scale Sweeney's (2009) simulated relative forces to the 19-Hz wave for comparison with Beason et al.'s (2009) plot of Force vs Repetition Rate (inset). We note that the maximum simulated force appears to level out at a repetition rate greater than 100 Hz (pps) as contrasted to Beason et al.'s measurement, which indicates that the asymptote is around 40 Hz (pps). We hypothesize that the difference is due to the fact that Beason et al.'s measurement is of a net force (leg pull) far from the stimulus and that Sweeney's simulation focuses on the theoretical reaction of a muscle directly stimulated. This difference leads us to conclude that the leg-pull measurements do not provide sufficient insight into the maximum forces delivered close to the stimulus location.

**Figure 2-6. Simulated Relative Force Normalized to TASER X26 Leg-Pull as a Function of Pulse Repetition Rate**

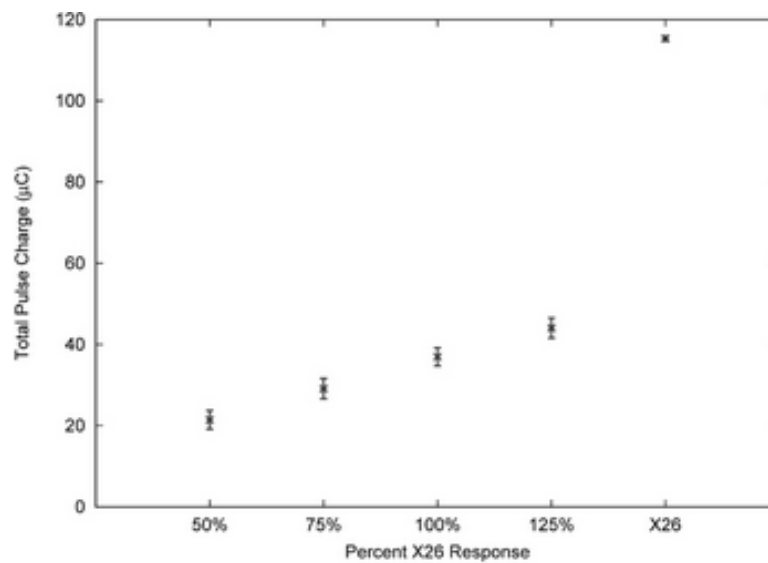
#### 4. Total Pulse Charge

Motor neurons are stimulated if the current that reaches the nerve exceeds the threshold for depolarization. Increases of the pulse charge (or current) above that level result in greater depth of effect, increasing the overall contraction strength via a volume effect. For therapeutic purposes, 5–10  $\mu\text{C}$  are generally used and are sufficient to generate contraction in the region local to the electrodes. Charge is adjusted to balance discomfort and the magnitude of contraction for the individual patient.

Before 2013, standard TASER<sup>®</sup> waveforms operated between 80 and 125  $\mu\text{C}$ . With introduction of the X26P with charge metering technology, the pulse per charge has been reduced to 63  $\mu\text{C}$  (TASER, n.d.). This reduction in pulse charge strongly indicates that unpublished testing or simulation has concluded that the body-wide incapacitation effects are within saturation at this level. IDA recommends that this assumption be confirmed by experiment. Beason et al. (2009) varied pulse charge and measured the normalized limb force of swine, demonstrating wide variation in leg-pull force as charge was increased from

60 to 320  $\mu\text{C}$  with 19 pps (results shown in Figure 2-3(c)). The researchers fit the data to a weakly increasing line, but the fit is poor ( $R^2 = 0.116$ ). The leg-pull force may be saturated at this point, or it may be continuing to increase slowly; however, the data are not clear enough to distinguish.

Comeaux et al. (2013) also explored leg-pull contraction force as a function of pulse charge, specifically varying pulse charge to produce set percentages of the effect observed using the TASER X26 waveform. As shown in Figure 2-7, 100% of the limb muscle contraction force is achieved using 40- $\mu\text{C}$  square waves at 40 Hz, and the relationship between effect and pulse charge appears to be linear in this regime. However, based on physiology of the human body, muscle contraction force must saturate at some value of pulse charge.

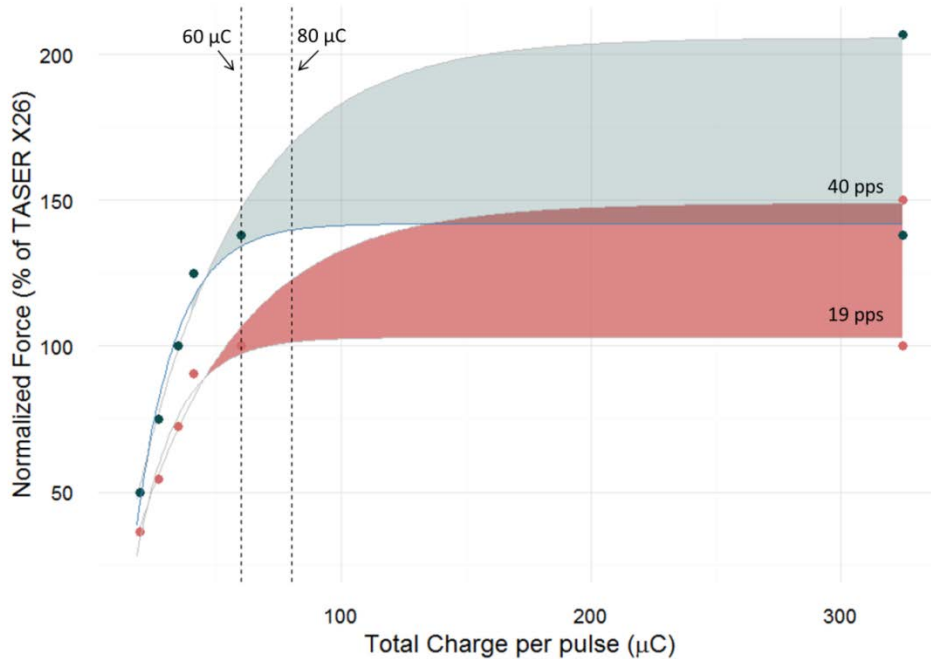


Source: Comeaux et al. (2013, 1029).

Note for Figure 2-7: The pulse charge of the square wave was varied to achieve set percentages of the limb force using the X26 waveform (115  $\mu\text{C}$ ). A linear relationship is observed in this regime.

**Figure 2-7. Total Pulse charge vs Percent X26 Response**

To explore the potential saturation point of the leg-pull force as a function of pulse charge, IDA combined the data from Comeaux et al. (2013) using 40 pps and varying pulse charge from 19.3 to 40.9  $\mu\text{C}$  and the data from the Beason et al. (2009) using 19 pps and varying pulse charge from 60 to 325  $\mu\text{C}$ . To combine the two data sets, IDA used scaling between the different data sets, as found in Beason et al. (i.e., a 42% increase in contraction force as repetition rate was increased from 20 to 40 pps). Figure 2-8 shows the results, with the bands representing a conservative (slope = 0) and generous interpretation (slope = 0.29Q) of the data reported in Beason et al. The accuracy of this extrapolation is limited by the confounding factors between the different experiments such as overall duration of stimulation and location of electrodes (which varied between the experiments).



Note for Figure 2-8: Combining the data from Beason et al. (2009) (19 pps and varying Q from 60 to 325  $\mu\text{C}$ ) and the data from Comeaux et al. (2013) (40 pps and varying Q from 19.3 to 40.9) and scaling the 19 pps. data sets up and the 40 pps down according to the measured scaling in Beason et al., we estimate that the contractile effect as observed in the pig leg-pull experiments saturates between 100 and 150  $\mu\text{C}$  for 40 pps and between 60 and 125  $\mu\text{C}$  for 19 pps. The upper estimates come from accepting the fit reported to the data in Beason et al., while the lower estimates come from assuming saturation around 60 pps for 19 pps (as evidenced by TASER Corporation's decision to set the level there, and the conservative interpretation of the data presented in Figure 2-3(b)). The dashed lines indicate the levels used by the AFRL study. The intersection of the dashed lines with the bands indicate levels used in the AFRL report and are reported in Table 2-1.

**Figure 2-8. Extrapolated Bands of Normalized Force as a Function of Charge per Pulse**

Note that the AFRL study used 60 or 80  $\mu\text{C}$  at 19 and 40 Hz, as shown by the vertical dashed lines in Figure 2-8. Table 2-1 shows the percentage of X26 effect according to the maximum and minimum estimates produced by IDA at each of the combinations of waveform parameters.

**Table 2-1 The Intersection of the Waveform Parameters Used in the AFRL Study with the Maximum and Minimum Percentage of X26 Estimates Produced by IDA**

Charge ( $\mu\text{C}$ )	Pulse Repetition Rate (pps)	Percent of X26 Effect
60	19	97%–106%
60	40	135%–147%
80	19	101%–122%
80	40	140%–170%

In McDaniel et al.'s (2005) experiment exploring the risk of ventricular fibrillation due to EMI, total pulse charge was significantly increased using the standard X26 complex pulse shape to identify the safety margin. The stimulus was delivered to swine in 5-sec. intervals at 19 pps. Total pulse charge in this experiment exceeded 2,000  $\mu\text{C}$  and was delivered across the thorax with no documentation of observed audible fractures.

## 5. Duration

Humans and swine have been tested or subjected in field use to durations exceeding 5 sec. Retrospective studies (e.g., Jauchem 2015) have looked at multiple or extended use of TASER X26 weapons against human targets, while controlled studies have exposed humans to up to 45 sec. of X26 stimulus (dorsal and ventral application,  $n = 18$  (e.g., Ho, Dawes, and Miner 2009)).

Swine have been tested up to 3 min. with continuous exposure to X26-like stimulus or in on-and-off cycles of the same with ventral application of the probes. Spinal compression fracture was not identified during any of these studies; however, the pigs were stimulated ventrally as opposed to the direct application on the back during the AFRL experimentation (Jauchem et al. 2009, Werner et al. 2012).

The effect of duration in the AFRL swine report is significant since fractures were observed in the first 3 sec. for a 40-pps stimulus and between 20 and 30 sec. for a 19-pps stimulus. This observation indicates that the effect is not due to initial muscle contraction levels alone, but to some factor introduced by duration. Based on the available literature, IDA concludes that the effects of duration are too complex to understand without significant modeling and experimental data collection efforts.

Therapeutic electrical stimulation can be used on the time scale of minutes, with no reported negative effects, although biphasic waveforms must be used to prevent excessive deposition of charge on the skin.

## D. Discussion

Our analysis of the available data has identified two main waveform parameters that have significant effect on the muscle force exposed to the EMI dose: charge per pulse and pulse repetition rate. Using the plot shown in Figure 2-8, it is possible to fit the force vs. charge data for various frequencies:

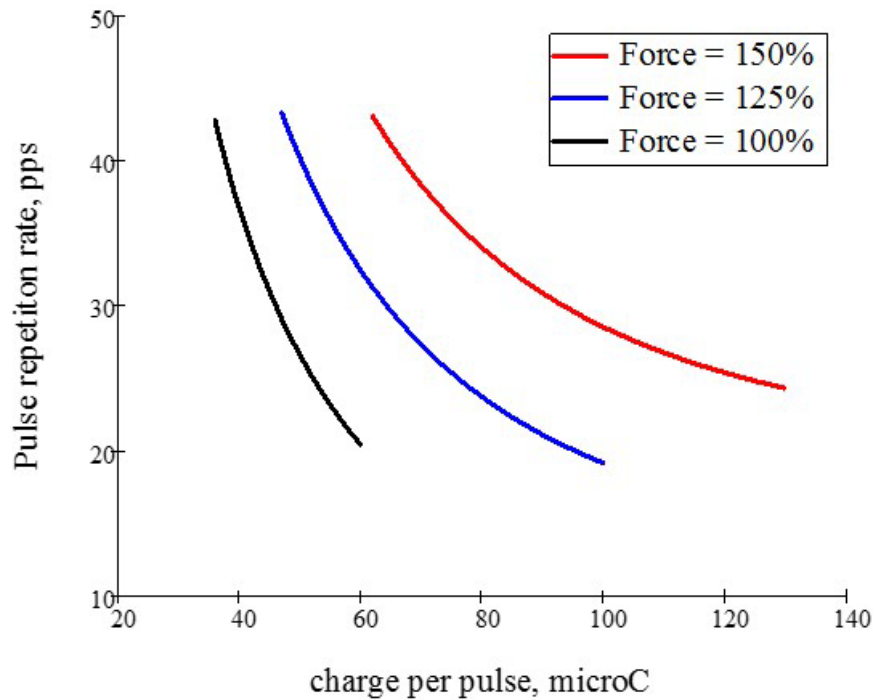
$$F(\omega, q) = 150f(\omega)(1 - e^{-.11 - .02q}),$$

where  $F(\omega, q)$  is the normalized force (as previously, the normalization is done with respect to the leg force produced by the X26 waveform),  $q$  is the charge per pulse,  $f(\omega)$  is the function that accounts for the effect of frequency on the saturation force, as shown in

Figure 2-3b. At 20 pps  $f(20) = 1$ , at 40 pps  $f(40)=1.42$ , and between these frequencies, this function takes the following linear form:

$$f(w) = 1 + \frac{.42}{20}(w - 20).$$

This formulation allows one to build contour plots that show combinations of pulse per charge and frequencies for various levels of normalized force. Figure 2-9 shows an example of such a plot.



Note for Figure 2-9: Contours of waveform parameters corresponding to a normalized level of muscle force. The risk of injury can be obtained by an inverse analysis (see Section 5)

**Figure 2-9. Normalized Force Contours (Based on Leg-Pull Data)**

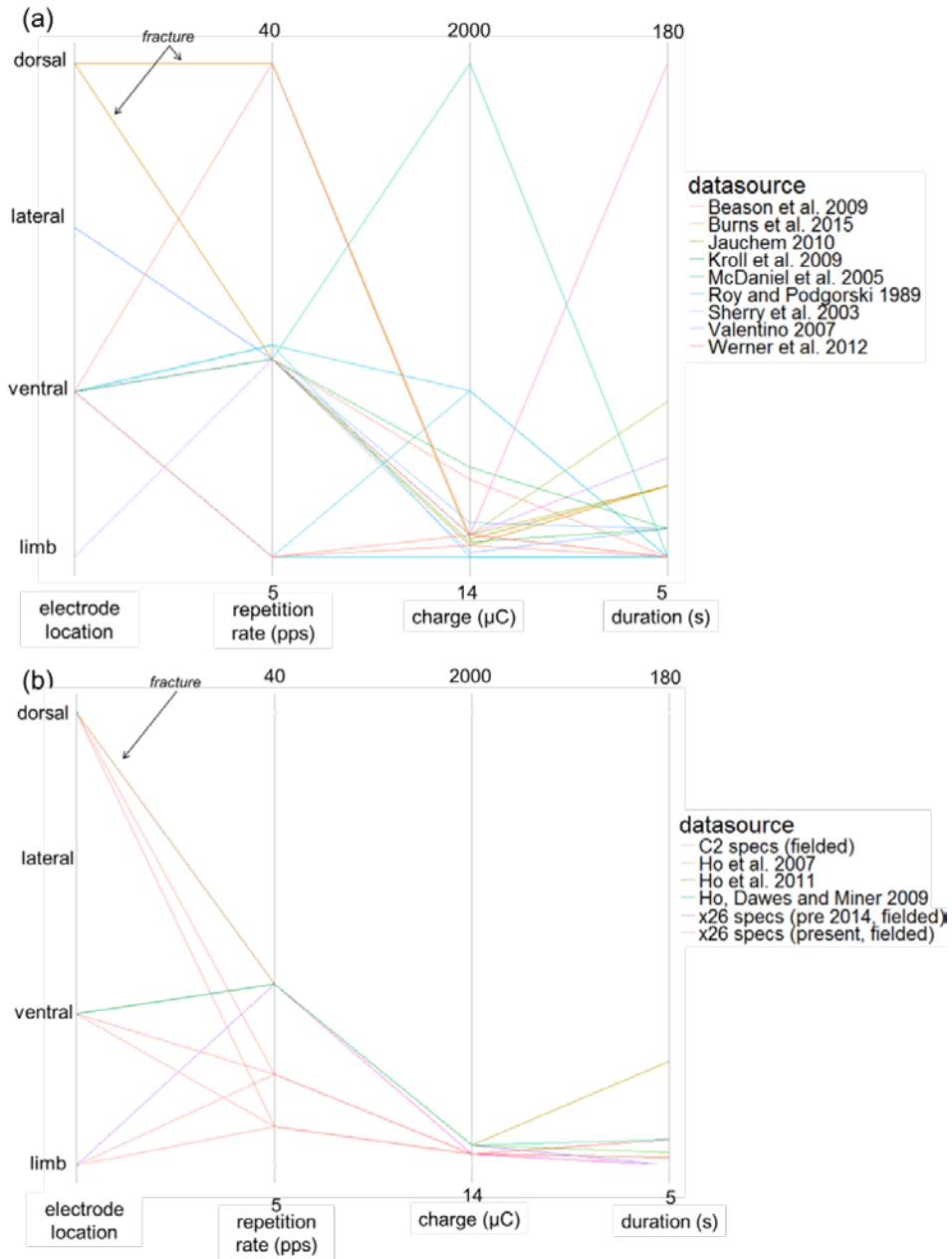
Note, however, that as discussed previously, the leg-pull force may not be representative of tension force in the spine muscle. To investigate the effect of waveform parameters on the spinal fractures, such a plot should be based on the spine muscles' forces. More generally, to understand the relationship between these waveform parameters (including duration) and contractile force and to take into account probe location, such plots should be based on the muscles local to the stimulus.

To wrap up the discussion, in Figure 2-10, we depict the space of tested EMI conditions and whether or not fracture occurred. The existence of a fracture in swine appears to be largely driven by electrode location (perhaps in combination with waveform details) since swine have been tested over many conditions with no observed fracture injuries,

except for those experiments with dorsal application. Aside from the AFRL 2015 report, we have only found published documentation with ventral, lateral, or limb application to swine. Humans have similarly only experienced observed fracture (albeit at a nearly negligible rate) with dorsal application. However the tested parameter space for humans is much smaller than that for swine.<sup>6</sup> On the other hand, the low rate of fracture is extremely significant statistically as the number of training exposures to the back is estimated to be nearly one million (Brewer and Kroll 2009). Nonetheless, the risk of SCF to humans remains unknown if the parameters are altered beyond the tested regions.

---

<sup>6</sup> We did not plot the therapeutic regime, which exceeds the EMI regime in duration and repetition rate, but in combination with much lower pulse charge.



Note for Figure 2-10: In (a) we show the known parameter space for swine testing based on data found in the literature. The conditions causing observed fracture are all within the non-fracture parameter space, except for electrode location (dorsal application). We found no sources of controlled experimentation in swine before the AFRL 2015 report (Burns et al.), which used a dorsal application. In (b) we show the same plot for humans, using data from known TASER<sup>®</sup> specifications or published experiments. In the case of humans, the conditions that caused fracture were also dorsal application only and overlap with conditions that were safe in the vast majority of exposures. In the case of human data, note that there is a large sample size in the dorsal application condition (due to field and training use) and only two fractures observed, whereas with swine, there was only one data set using reporting dorsal experimentation (AFRL).

**Figure 2-10. Parallel Coordinates Plot of Known, Experimentally or Field Tested Parameters in (a) Swine and (b) Humans**

### 3. Vertebral Loading and Injury

---

The occurrence of a SCF depends on factors of the stimulus and on the relative strengths of muscles and vertebrae. In Chapter 2, we established the existing data sets and where the AFRL data fit in the parameter space of effects. We do not, at this time, have experimental data to support a likelihood estimate of SCF in humans due to various combinations of the waveform parameters. In the absence of these data, we look at the relative strength of muscle contraction forces produced under varied conditions on the spine and the threshold forces (as measured *in vitro*) to produce fracture to understand whether SCF is an area of concern for EMI use.

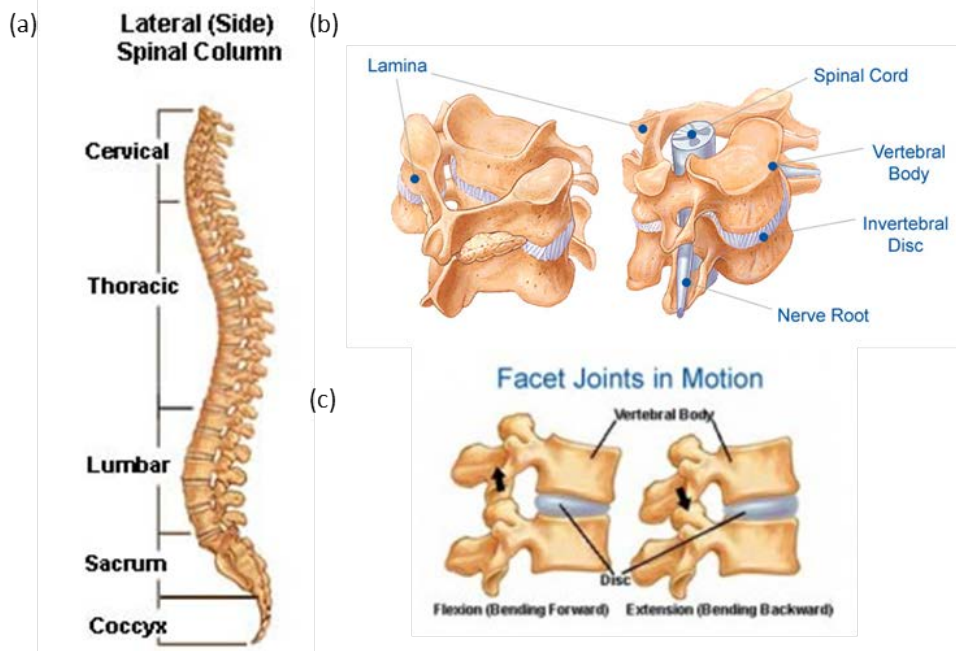
#### A. Human Spine and Back Musculature

The human spine consists of four sections: cervical, thoracic, and lumbar, and sacral, as shown in Figure 3-1(a). A diagram of an individual vertebra is shown in a neutral position in Figure 3-1(b) and under bending conditions in Figure 3-1(c). The vertebrae are numbered in ascending order from the skull and identified based on the region (i.e., C1-C7 in the cervical, T1-T12 in the thoracic, and L1-L5 in the lumbar region).

Individual vertebra are loaded by multiple muscles adhered to tendons at the spinal processes. The deep back muscle groups relevant to motion and stability are the (1) erector spinae group, (2) transversospinal group, and (3) short segmental muscle groups, as shown diagrammatically in Figure 3-2.

Figure 3-3 demonstrates the complexity of coordination in the human back, depicting attachments of the erector spinae and transversospinal group of muscles to a particular vertebrae (T9). The forces produced on a given vertebrae depend on the contractile state, orientation, and lever arm of each of the muscles shown.

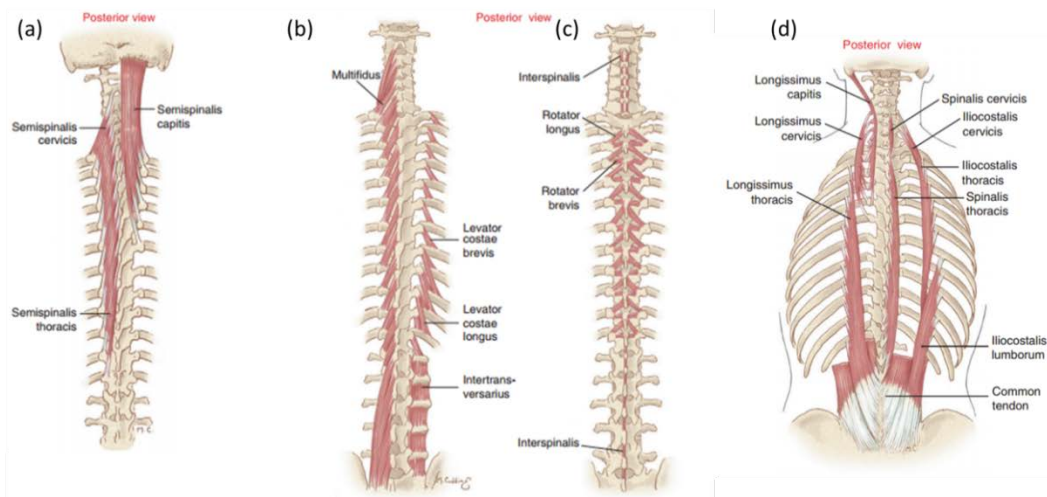
Figure 3-4 shows the spatial orientation of the muscle's line of force for the intrinsic muscular stabilizers in the back. Summing all the forces on a given vertebra (even statically) is a task that requires complex geometry and significant computational effort. Luckily, such models (biomechanical or finite element) exist and can be leveraged for further understanding of the compressive loads on the spine. In Section 3.B, we discuss experimental measurements and computational methods to estimate such forces.



Source: Bridwell (2016a, 2016b).

Note for Figure 3-1: (a) the side view of the human spine, with the cervical, thoracic, lumbar regions, sacrum and coccyx identified; (b) a single vertebra showing the structures of the human vertebra; and (c) compressive conditions of flexion and extension.

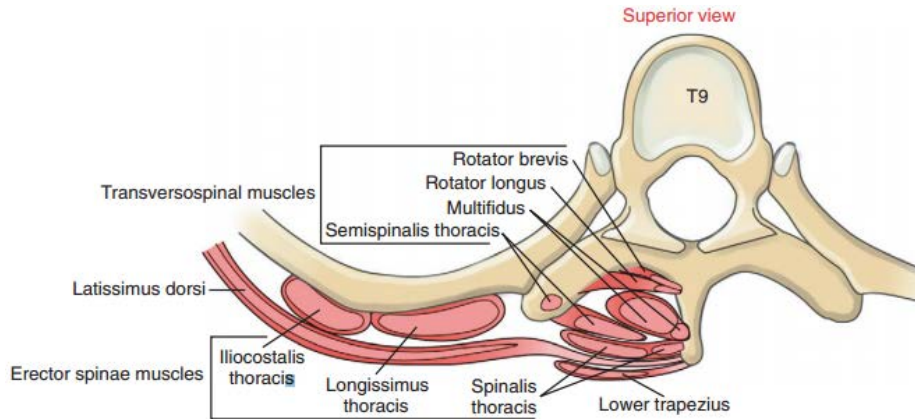
**Figure 3-1. The Human Spine**



Source: Neumann (2010) (modified from Luttgens and Hamilton (1997)).

Note for Figure 3-2: (a) a posterior view showing the more superficial semispinalis muscles within the transversospinales group; (b) a posterior view showing the deeper muscles within the transversospinal group (multifidi on entire left side of (b); rotatores bilaterally in (c)). The muscles within the short segmental group (intertransversarius and interspinalis) are depicted in (b) and (c), respectively. Note that intertransversarius muscles are shown for the right side of the lumbar region only; (d) the muscles of the erector spinae group. For clarity, the left iliocostalis, left spinalis, and right longissimus muscles are cut just superior to the common tendon.

**Figure 3-2. The Human Spine: Deep Back Muscle Groups Relevant to Motion and Stability**



Source: Neumann (2010).

Note for Figure 3-3: The short segmental group of muscles is not shown.

**Figure 3-3. Cross-Sectional View through T9 Highlighting the Topographic Organization of the erector Spinae and the Transversospinal Group of Muscles**

A) Intrinsic muscular stabilizers	B) Spatial orientation ( $\alpha$ ) of muscle's line of force
Intertransversarius and interspinalis (cross 1 junction)	Percent of force directed: Horizontal ( $F_H$ ) Vertical ( $F_V$ ) $F_H = 0\%$ $F_V = 100\%$
Semispinalis cervicis (crosses 6-8 junctions)	$\alpha = 15^\circ$ $F_H = 26\%$ $F_V = 96\%$
Multifidus (crosses 2-4 junctions)	$\alpha = 20^\circ$ $F_H = 34\%$ $F_V = 94\%$
Rotator longus (crosses 2 junctions)	$\alpha = 45^\circ$ $F_H = 71\%$ $F_V = 71\%$
Rotator brevis (crosses 1 junction)	$\alpha = 80^\circ$ $F_H = 98\%$ $F_V = 17\%$

Source: Neumann (2010).

Note for Figure 3-4: A): The lines of force of muscles are shown within the frontal plane; B): The spatial orientation of the lines of force of each muscle is indicated by the angle ( $\alpha$ ) formed relative to the vertical position. Note that the muscles illustrated exist throughout the entire vertebral column. Their location in the figure is simplified for the sake of clarity.

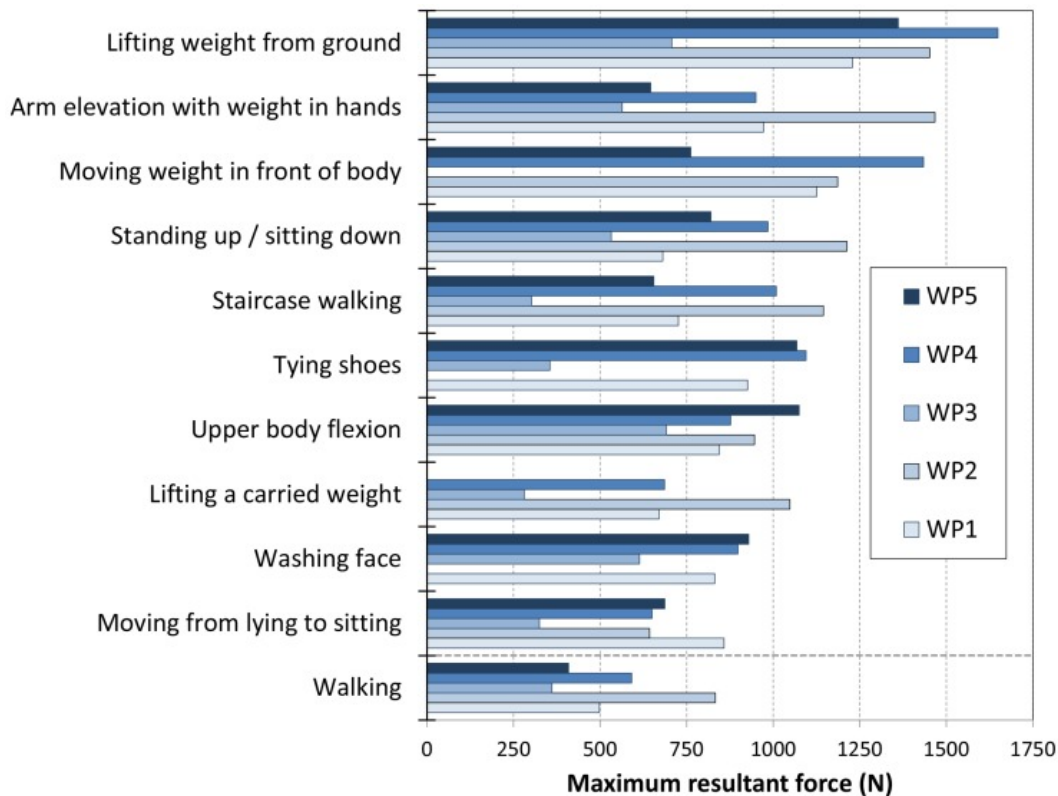
**Figure 3-4. Diagrammatic Representation of the Spatial Orientation of the Lines of Force of the Intrinsic Muscular Stabilizers**

## B. Spinal Loading through Everyday Activities

The human spine can withstand significant compressive loading without fracture due to muscle contraction resulting from everyday activities. Due to the prevalence of low back injury, the lumbar spine is most well studied for understanding compressive loading. Here, we discuss results of direct *in vivo* measurements (using implants or pressure sensitive needles inserted into the spine) and simple biomechanical models to compare them to *in vitro* estimates of compressive strengths of the vertebrae.

### 1. Measurement and Prediction of Loading

Five post-operative vertebral body replacement (VBR) patients participated in a study to measure loads telemetrically on their VBR. Approximately 1,000 combinations of activities and parameters were measured. Figure 3-5 shows the top 10 resultant forces on the VBR (located at L1 or L3 in each of the patients).



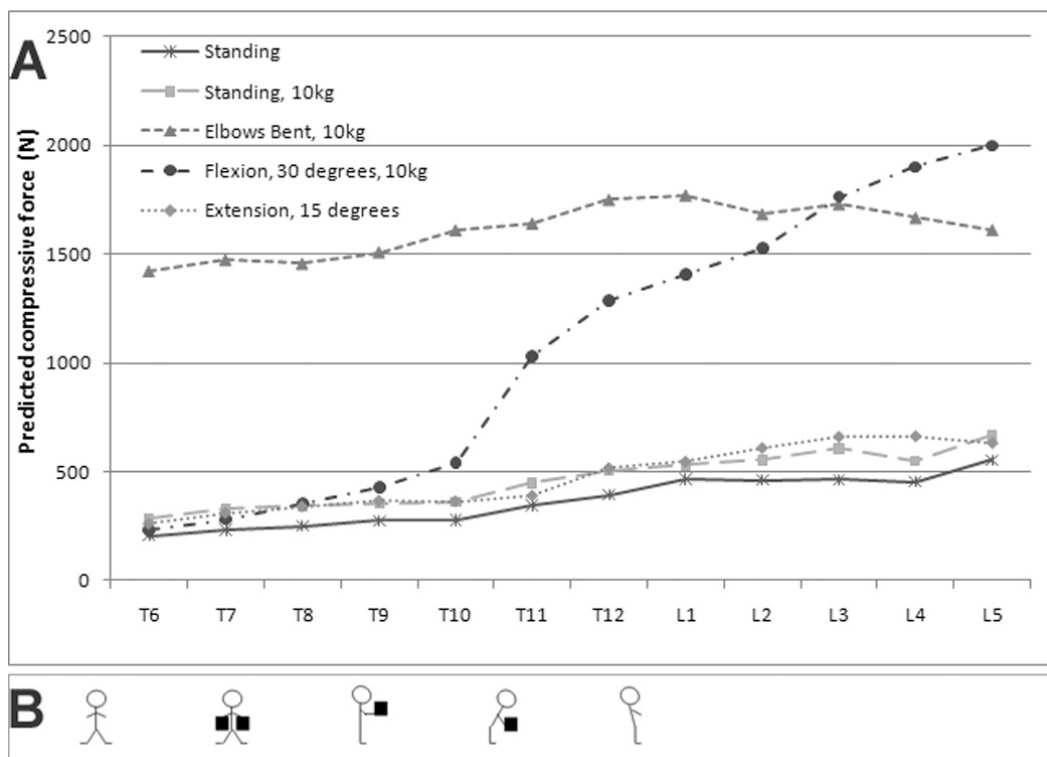
Source: Rohlmann et al. (2014, Figure 1).

Note for Figure 3-5: The maximum forces for the five patients are shown. For comparison, maximum forces for walking are given.

**Figure 3-5. Ten Activities with the Highest Maximum Resultant Force**

We note that lifting a weight (4–10 kg) produced the highest vertebral loads, exceeding 1250 N in three cases, but that tying shoes, standing up or sitting down, and walking up a set of stairs each can produce loads exceeding 1000 N.

Biomechanical models of the human spine under loading conditions are also useful for compressive force estimates. Iyer et al. (2010) developed a quasi-static stiffness-based biomechanical model that can be used to calculate loads on the thoracic and the lumbar spine (see Figure 3-6). The model was validated with existing experimental data that consisted of pressure-sensitive needle insertion into the disc space (Polga et al. 2004).



Source: Iyer et al. (2010, 855).

Note for Figure 3-6: Model compressive forces depended strongly on the predicted task. This figure depicts task-dependent changes in compressive force (A). The tasks modeled in this figure are also shown (B). From left to right, these tasks are standing, standing with 10 kg (5 kg on each arm), lifting 10 kg with elbows bent, 30 deg. flexion with 10 kg, and 15 deg. of extension.

**Figure 3-6. Forces on the Vertebral Bodies**

The largest compressive forces were predicted for T6-L5 and exceed 1500 N in the most stressing case of lifting a weight (10 kg) with elbows bent. These predictions are consistent with the measured values from Rohlmann et al. (2014). These activities represent fairly common activities, and few individuals would claim maximal exertion to achieve such levels. However, the maximum muscle capacity of the human back remains unclear. To provide insight into the maximum capacity, we turned to extreme external loads

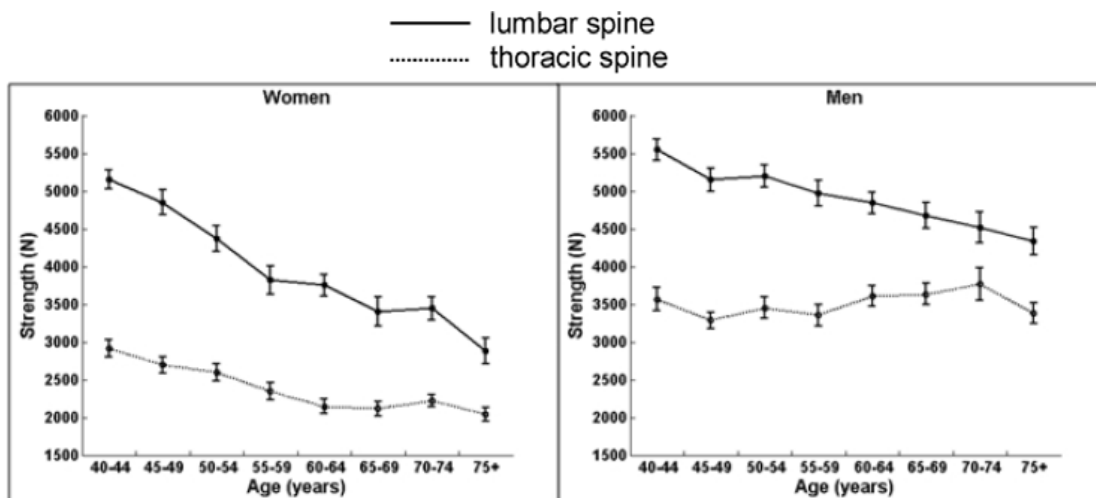
to understand how much stress the back muscles can produce and, in turn, how much stress the vertebra can withstand.

Cholewicki, McGill, and Norman (1991) used simple force balance equations to estimate the compressive forces on the lumbar spine during extreme weight lifting. Estimates of disc compression at the L3-L4 vertebra ranged from 5844 N for a female weight lifter dead lifting 155 kg to 17,192 N for a male weight lifter dead lifting 275.8 kg.

## 2. Measured Vertebral Compressive Strength

The value of such measurements and predictions of vertebral loading is only useful in the context of the compressive strength of the vertebrae under such pressure. We found two such studies performed on cadavers. Limitations of this method include changes to the structural integrity of the vertebrae upon embalming and selection bias toward the elderly for sample. Nonetheless, the data provide a useful bench mark.

Samelson et al. (2012) found compressive strength of the thoracic and lumbar spine to be approximately 5000 N (lumbar) and 3000 N (thoracic) for healthy middle-aged women and 5500 N (lumbar) and 3500 N (thoracic) for healthy middle-aged men. The compressive strength of the lumbar spine is found to decrease with age, more sharply for women than for men, due to effects of menopause on bone density. Male thoracic spine compressive strength remained relatively constant from age 40 to 75+ as shown in Figure 3-7.

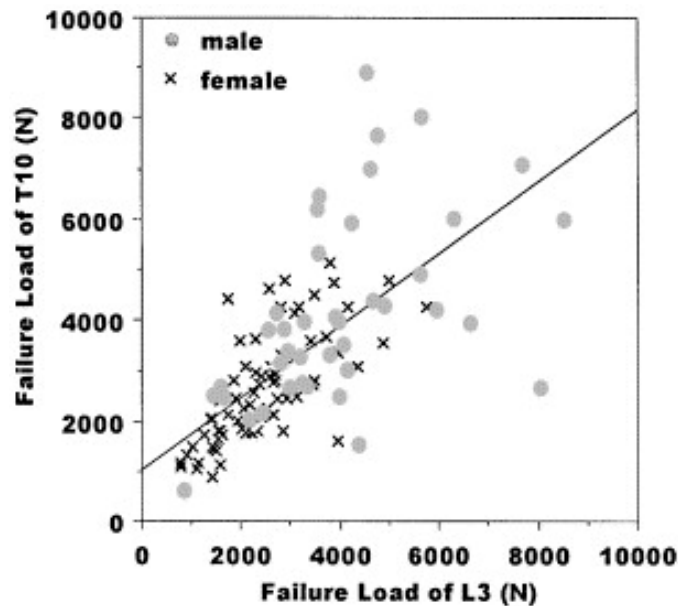


Source: Samelson et al. (2012, Figure 2A).

**Figure 3-7 Averaged Strength of Thoracic (T8-T10) and Lumbar (L3-L5) Strength for Women and Men of Various Ages**

Bürklein et al. (2001) performed similar measurements (average age of subjects was elderly) and found the failure load of thoracic vertebra T10 (lumbar vertebra L3) to vary

from 9500 (8500) N to less than 1000 N for men, and from 5000 (6000) N to less than 1000 N for women. See Figure 3-8.



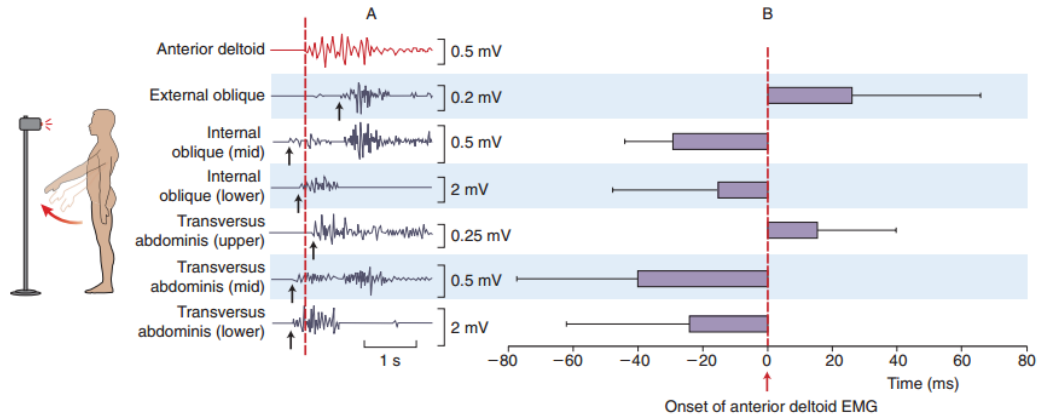
Source: Bürklein et al. (2001, 582).

**Figure 3-8. Correlation of Vertebral Failure Loads of T10 and L3 in Both Genders**

### 3. Discussion

Based on the relative loads and strengths, every day activities would produce significant threat to vertebrae only at the weakest end of the spectrum. However, extreme conditions (e.g., those produced by weightlifters) that exceed measured compression strengths by multiple factors indicate that the fracture prediction may include more than a comparison of force-balanced loads and compressive strengths.

Indeed, unconscious active muscle coordination is likely to play a role. The abdominal muscles play a large role in stabilizing the spine and activate in response to certain body movements ahead of back muscle contraction, as shown in Figure 3-9. Electromyographic (EMG) measurements of muscle activation were used by Urquhart, Hodges, and Story (2005) to track the abdominal contraction patterns during controlled upper limb movement (measured by contraction of the anterior deltoid). The internal oblique and mid and lower transversus abdomini muscles were activated tens of milliseconds before the anterior deltoid. The researchers hypothesize that such anticipatory muscle contraction is used to minimize counter-movements of the trunk during strenuous activities, potentially protecting the vertebrae from damaging shear forces. Other research shows that the lumbar multifidi (stabilizers of the lumbar spine, especially in the lower segments) are similarly recruited early in stressing perturbations to the lumbar spine. (Neumann 2010).



Source: Neumann (2010) (redrawn from Urquhart, Hodges, and Story (2005)).

Note for Figure 3-9: (A): The EMG responses are shown from selected abdominal muscles as a healthy person rapidly flexes his arm after a visual stimulus. The different onset times of EMG signals from the abdominal muscles (vertical dark arrows) are compared with the onset of the EMG signal from the anterior deltoid (red), a shoulder flexor muscle; (B): The overall results of the experiment are shown, averaged across 110 trials in 11 healthy subjects.

**Figure 3-9 EMG Responses (Intensity and Onset Time) during Arm Flexing**

The relevance of this type of muscle contraction optimization is that it is unavailable to EMI targets (and epileptics, tetany, and shock therapy patients) since muscle contraction is nonselective, activating all muscles within the region of effect at the same time. These effects may prove significant as muscle contraction is increased to saturation levels.

### C. Epilepsy, Tetany, Shock Therapy, and EMI

The incidence of vertebral fractures induced by shock-therapy-driven muscle contraction and epileptic seizures has been accepted for a long time. Vasconcelos (1973) found a 15% incidence of spinal fracture evidence in patients who had grand mal seizures but no history of back pain or injury. Estimates of prevalence vary widely, ranging from approximately less than 1% to 66% (Kelley 1954; Finelli and Cardi 1989). In contrast to epileptic cases, secondary trauma was easily excluded in shock therapy patients who were treated lying in bed. In a study in Lancaster, England, in the 1940s and 1950s, 2,200 patients had 37,000 convulsions induced, which resulted in 21 cases of diagnosed vertebral fractures, most of which occurred in the thoracic spine. Notably, the least flexible region of the spine, T4-T7, experienced the highest incidence of fracture, and most fractures did not occur on the first convulsion.

None of the spinal fractures required surgical support or repair. They self-resolved. Two primary types of fracture were observed. The first, termed a wedge fracture, was hypothesized to be due to the initial spasmodic flexion. The second, termed a disc reperussion fracture, involved a penetration of the vertebral body by the intervertebral disc and was hypothesized to be due to severe compression, most likely during spasmodic arching of the back (Kelley 1954). Kelley also examined records of epileptic-seizure-induced

fractures and noted that the fractures occurred lower in the thoracic region (T8-T12). The epilepsy cohort was not controlled for secondary injury. Interestingly, Kelley speculated that the difference in spinal location of epileptic and shock therapy fractures may be due to differences in pelvic posture between standing and reclining patients, indicating that initial posture may be significant.



## 4. Surrogate Framework for EMI-Induced Spinal Compression Fractures

### A. Generalized Surrogate Framework

In the most general terms, a framework for using a surrogate system to predict injury risk to humans consists of four systems plus a transfer function, as depicted in Figure 4-1. On the far left side of Figure 4-1 is the surrogate experimental system in which the stimulus (insult or dose) is applied to a surrogate for the live-human (mannequin, animal, cadaver, or a test device such as a clay form or test plate). Measurements on the surrogate characterize the surrogate response. A surrogate system model, second from left in Figure 4-1, can be used to compute elements of the surrogate response less accessible to measurement. Next, a transfer function relates the derived surrogate system response to the human response under equivalent stimulus. The human model, second from right in Figure 4-1, computes the remainder of the human response including risk of significant injury (RSI), which then stands in for the human response that would have been observed in an end-to-end live human experiment with the same stimulus, shown at far right in Figure 4-1.

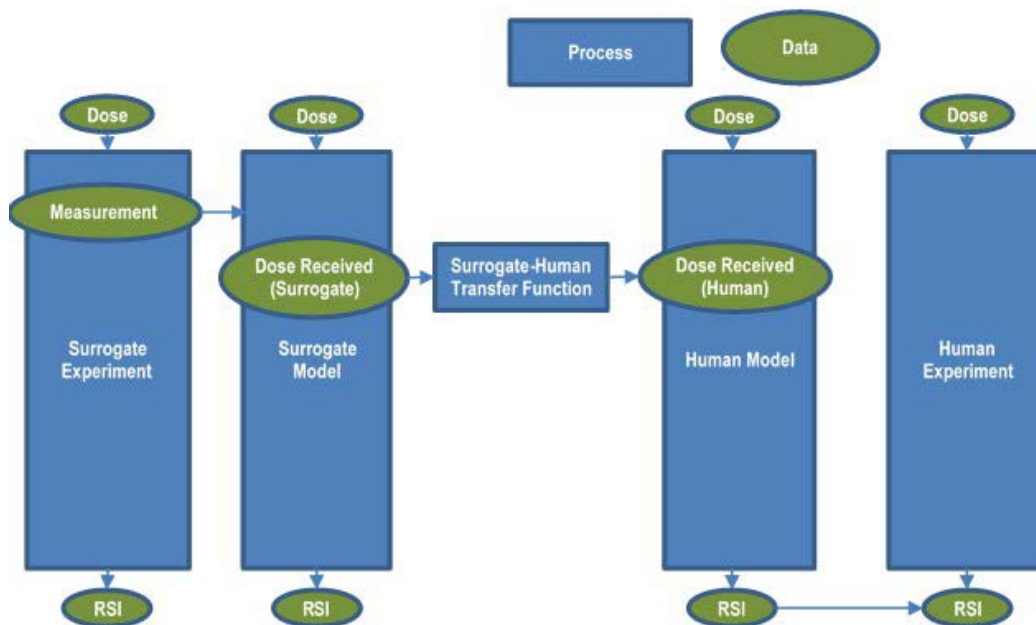
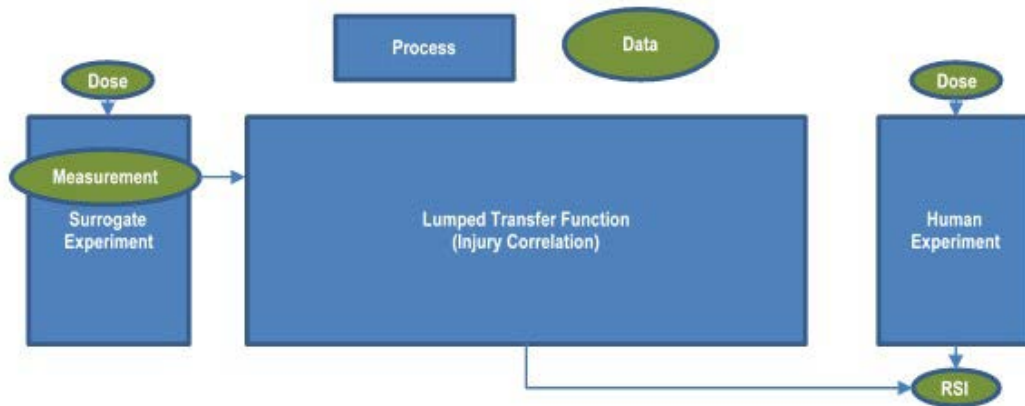


Figure 4-1. Surrogate Framework

In principle, the surrogate model and human model could be grouped with the transfer function and thought of, in aggregate, as an overall transfer function or mapping from surrogate measurement to live-human RSI, as shown in Figure 4-2. A lumped transfer function such as that would likely be a fully empirical correlation, potentially difficult to develop and validate. Nevertheless, the construct is useful because it clearly shows the need for an unambiguous mapping between surrogate measurement and RSI. If the surrogate measurement does not correlate well with RSI, no models of any fidelity that take the surrogate measurement as input will usefully predict the RSI. Separating the surrogate and human models from the transfer function breaks the otherwise opaque empirical mapping into physically motivated causal blocks that have potential for independent development and validation. The choice of models sometimes embodies a tacit hypothesis about the injury mechanism. For instance, a clay form can be modeled to infer energy deposition from the clay imprint of a blunt impactor, which embodies a hypothesis that spatial distribution of projectile energy is the primary determinant of injury. In such a case, the transfer function and human model might be lumped into an empirical correlation between energy as distributed over an area of effect on the clay form and RSI.



**Figure 4-2. Lumped Transfer Function Construct**

The highest fidelity response would be generated by using direct live human experiments. For ethical or logistical reasons, live human experiments are often infeasible. If stimulus-to-RSI human modeling were available, no surrogate would be routinely necessary, but it might be needed to build or validate such a model. However, in many cases, such models do not exist. Thus, we are forced to rely on surrogate systems. Validation of all of the framework components is also a challenge. How can the framework's representation of the human be validated without the direct human experimentation, whose infeasibility motivated the development of the framework in the first place? While some extrapolation from tested conditions to untested conditions is nearly inevitable, confidence in extrapolation is built by using physics- and physiology-based models, where possible, in

conjunction with testing over a variety of conditions that attempt to approximate or bracket field conditions. Also, even if end-to-end experiments are not possible, some models can be built and validated in a hierarchical fashion, giving confidence in their building blocks. Ultimately, field experience with the real version of the modeled system should be analyzed to confirm that the model behaves as expected.

The following criteria are necessary for a predictive surrogate framework:

- Experimentally feasible surrogate,
- Measurable experimental response,
- Input to the transfer function that is either measurable or derived from validated model,
- Unambiguous transfer function (input surrogate response maps to only one human response with enough information to prescribe RSI),
- Validated transfer function, and
- Validated model that relates human RSI to the output of the transfer function.

A surrogate with an identity map (identical responses) between surrogate response and RSI would obviate the need for modeling. For instance, if an animal were to experience the same injury risk as a human under the same circumstances, the surrogate framework could consist of experiments on that animal, with injury statistics used as a direct stand-in for human RSI.

It is important to have a conceptual causal model that links the stimulus to the injury to ensure the choice of relevant measurements and models. A causal—as opposed to a correlative—model should also be more robust to extrapolation beyond validated conditions. The function of the surrogate framework is clearest when a similar causal chain operates in the surrogate system through the point of measurement so that any human-unique causality resides in the human model portion of the framework.

A perfect surrogate would be one in which the surrogate and human systems share a causal chain through the point of measurement, with an identity-map transfer function to the human system at a point from which RSI modeling is readily accomplished. In theory, any surrogate system whose measurement preserves the differences between doses that lead to different injury risks could be used as the basis for an empirical injury correlation. Broad validation of such a correlation would be the challenge.

The maintenance of similarity in the surrogate and human systems (transfer function feasibility) and in human system modeling complexity requires a tradeoff. Consider Figure 4-3. If the total content of the causal chain is fixed at 100% and  $x$  and  $y$  represent

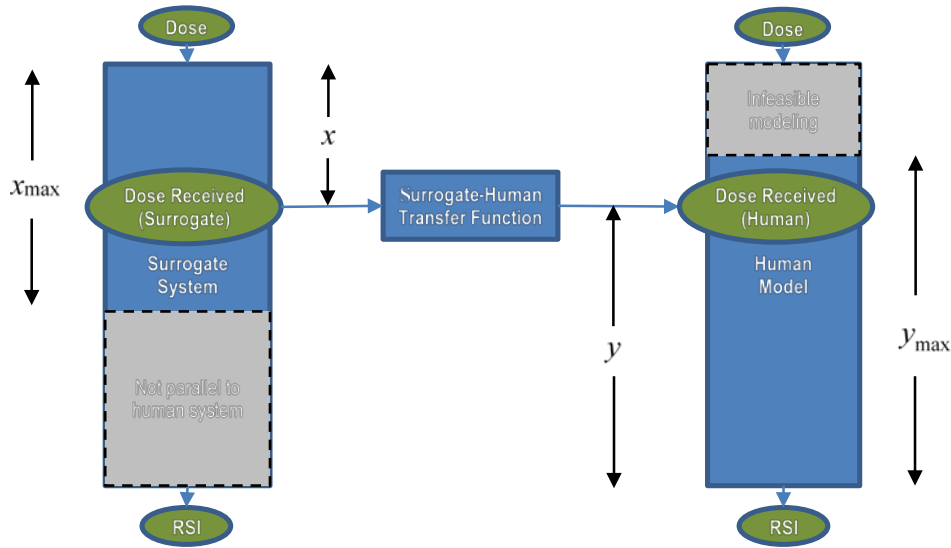


**Figure 4-3. Similarity/Modeling Complexity Tradeoff**

the fractions of the causal chain captured in the surrogate system and in the human system model, respectively, then  $x + y = 100\%$ . Any decrease in  $x$  must be offset by a corresponding increase in  $y$ . Increasing  $x$  corresponds to increasing reliance on the similarity of the surrogate and human systems. It presumes more parallel causal steps between the two systems. If  $x$  exceeds the point of relevant divergence between the surrogate and human systems, ( $x_{\max}$ ), a reliable transfer function becomes infeasible. Larger  $x$ , in general, requires more validation work to ensure causal parity between the two systems. In this sense, validation of the transfer function becomes more difficult as  $x$  is increased until it becomes impossible when the point of final causal parity is exceeded. On the other hand, as  $x$  increases,  $y$  decreases, meaning that the number of causal steps captured by the human model decreases and the human model complexity decreases. Typically, some maximum value of  $y$  ( $y_{\max}$ ) exists beyond which human system modeling is infeasible. A surrogate system approach is only feasible if the entire dissimilar portion of the causal chain can be modeled ( $y_{\max} \geq 1 - x_{\max}$ ).

## B. EMI-Induced Spinal Compression Fracture

EMI applies a time-dependent voltage across a pair of conductive barbs embedded in or otherwise adhered to the target's body. The basic causal chain follows. The electric potential difference generates an electric field, which activates muscle contractile responses. The muscle activation applies forces to bones via tendons, thus generating stress distribution in the bones. If the stress exceeds the fracture stress of the bones, they can break.

The detailed causal chain, however, has some complexities. The particular forces exerted by each muscle may depend on the EMI waveform, the current contractile state of

the muscle, positions of the surrounding joints, and the fatigue state of the muscles. Also, the human body posture is not static during the muscular excitation. The forces exerted on the bones change the angles of the joints, which then feeds back to change the forces on the bones.

Three basic considerations regarding proximate cause of fracture, each of which would influence the complexity of the model required to capture fracture risk, are as follows:

- **Material strength.** Does nominal bone strength account for the vulnerability to vertebral fracture or must material fatigue or damage accumulation be considered? Are preexisting degradation or other natural variation of material strength dominant factors in fracture occurrence?
- **Postural dynamics.** Does the bone stress exceed the fracture threshold in the static initial body configuration or must altered postures or body dynamics be considered to account for fracture risk?
- **Contraction time phasing.** Does ordinary uncoordinated muscle contraction lead to critical bone stresses or would these stresses require extraordinary synchrony or asynchrony of contraction due to chance, coordinated stimulation, or asymmetric muscle fatigue?

### C. Transfer Function for Electro-Muscular Porcine to Human Spinal Compression Surrogate

For our specific case of spinal compression injury in response to EMI dose, the pig may represent a useful surrogate if it parallels a complex part of the human injury causal chain not amenable to reliable modeling. For instance, if the muscular reaction to a particular EMI waveform is difficult to predict in humans but is measurable in pigs and if the anatomy and physiology of humans and pigs are sufficiently similar in terms of induced electric fields, nerve susceptibility to such fields, and muscular response to stimulated nerve activation, then pigs might be used effectively as a surrogate for human muscular response to EMI.

With respect to a general formulation of pig-human surrogate system, a tractable number of possible stages exist at which the pig system/human system responses can be correlated. To follow this progression, we show these stages in Figure 4-4. Each stage, at which a transfer function can, in principle, be established is indicated by the dashed arrows. Recall that as we discussed earlier, the transfer stage also delineates between the transfer function complexity,  $x$ , and the model complexity,  $y$ .

For example, the arrow on the far right in Figure 4-4 would suggest that it is possible to establish a transfer function that determines EMI doses that lead to fractures in a human spine by simply measuring EMI doses injurious to pigs. In this case, the complexity of the transfer function, “ $x$ ”, is at its maximum, while modeling effort, “ $y$ ”, is at the minimum.

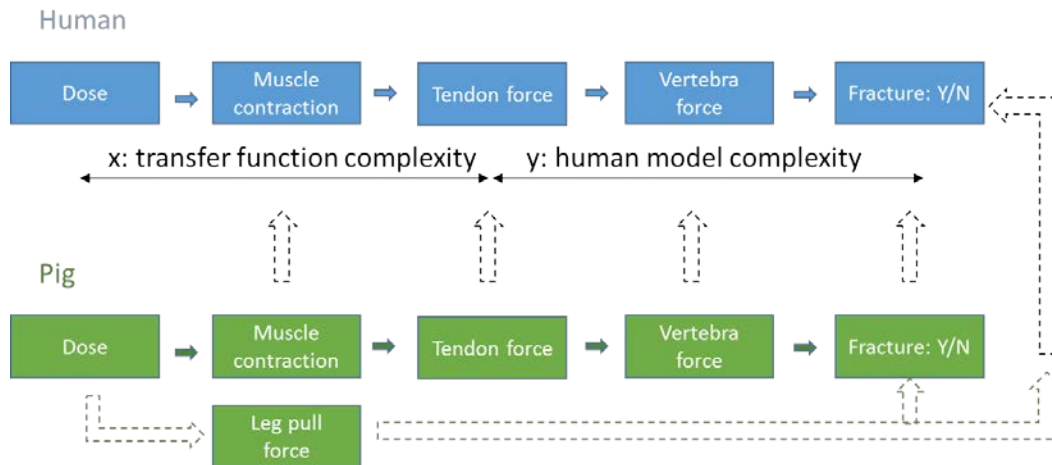


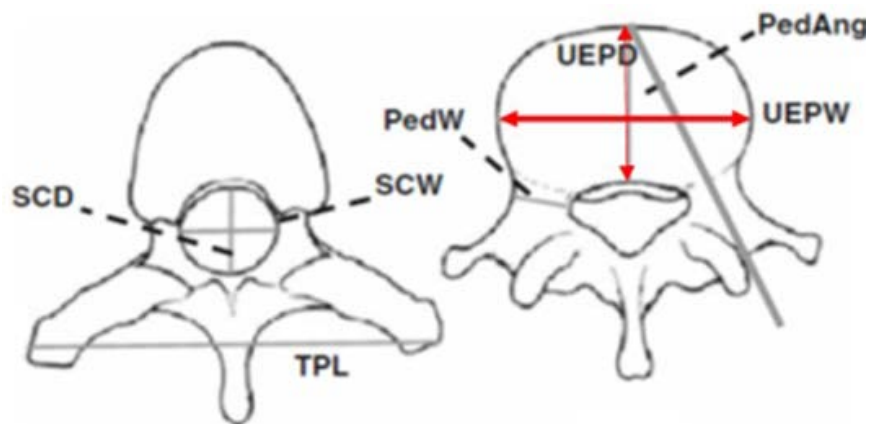
**Figure 4-4. Schematic Diagram of a General Pig-to-Human Transfer Function**

The following options describe the transfer functions stages in increasing order of reliance on human body-system modeling (increasing  $y$ ), corresponding to decreasing order of reliance on pig-to-human correlation (decreasing  $x$ ).

- Option 1: Direct correlation of RSI in pigs with those in human, as indicated by the transfer function error represented on the far right in Figure 4-4.** This transfer function requires an unambiguous mapping directly from the injury risk in pigs to that in humans. The existence of such a transfer function appears to be highly unlikely since it is predicated upon the assumption that the vertebral forces due to EMI doses and the critical (breaking) force in the vertebra in pigs and human are similar. We have found that this is not the case. Shown in Figure 3-7 are the data on vertebral strength in humans that were published in Samelson et al. (2012). While being a function of human age and being different for men and women, its magnitude is clearly above 2000 N. As reported in Mosekilde, Kragstrup, and Richards (1987), breaking strength in porcine vertebra is only about 850 N, suggesting that porcine vertebra would break at an applied force that is significantly lower.
- Option 2: Correlating vertebral force/stress.** This correlation would allow for differences in human and pig bone material [breaking] strengths but would require strong correlation between the forces/stresses experienced in human and porcine vertebral bones in response to the same EMI dose. The vertebral bone geometry and musculature differences, however, suggest that this assumption is

not realistic. We illustrate the differences in vertebral geometry in humans and pigs in Figure 4-5 and Figure 4-6.

Figure 4-5 shows the vertebrae geometry and associated letter notation for each vertebral dimension as measured in both human and swine. We pay particular attention to the dimensions of Upper End Plate Width (UEPW) and Upper End Plate Depth (UEPD), denoted by the red arrows. These parts of the vertebrae (in the thoracic region) support the stresses that caused the reported human spine fractures (Winslow et al. 2007; Sloane, Chan, and Vilke 2008). The geometrical differences in the human vs. porcine vertebrae structure are reported in Busscher et al. (2010), where the comparison for all the vertebra measurements are given.

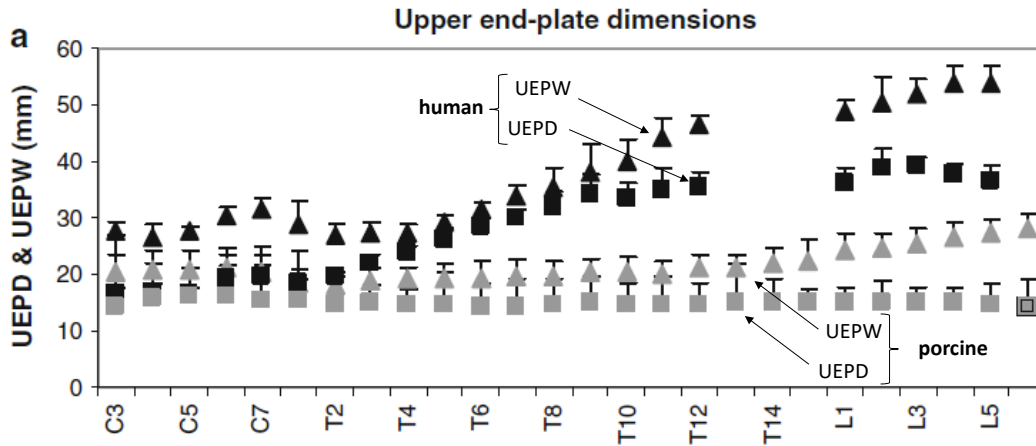


Source: Busscher et al. (2010, 1105).

**Figure 4-5. Anatomical Dimensions Measured per Vertebra**

Figure 4-6 shows a selected figure that demonstrates these differences for UEPD and UEPW. Note that the human T7-T8 vertebral depth and width exceeds those of porcine by more than 50%, which suggests that even if the forces are similar, the stresses in those bones are not the same. It is unlikely, therefore, that similar bone forces would lead to direct correlation of fractures in pigs and humans.

- **Option 3: Tendon forces.** This transfer function would require similar musculature response but would allow for bone geometry and material strength differences. In other words, electro-muscular stimulation would generate a similar level of tension in each muscle. The transfer function could account for the differences in muscle strength and geometry (insertion angle and so forth). A finite element model or other biomechanical model could then be used to predict bone stresses in humans as a function of tendon loading. An injury model of bones (fracture stress) would then generate an RSI. Experimental *in vivo* measurement



Source: Busscher et al. (2010, 1109).

Note for Figure 4-6: Error bars indicate positive standard deviation.

**Figure 4-6. Upper End-Plate Dimensions of the Human and Porcine Vertebra**

of individual muscle forces could be a challenge as could inference of muscle forces (using a porcine model) from external gross force measurements, particularly for overlapping effects of various core muscles.

Note that in the AFRL report, the measurements of the EMI dose were correlated with the acceleration of the muscle pull of the pigs' hind legs and, subsequently, with the spine fracture, as shown by the dashed green arrow in Figure 4-4. While this allows easier measurement of the porcine response, due to the ambiguous relationship between leg-pull force and individual core muscle forces and their time phasing, construction of a validated and general transfer function becomes practically impossible.<sup>7</sup>

- **Option 4: Nerve impulse.** This transfer function would require an identical electrical stimulus that would similarly excite porcine and human nerves, but it would not rely on similarity in muscle force response to nerve impulses. In particular, this option might eliminate challenges of differences in muscle size, structure, and dynamic postural changes in the two species. The human model in this case escalates in complexity from a biomechanical model to one involving nerve-muscle activation, fatigue, and possibly body dynamics. Advances in electrophysiological modeling, such as those referenced in Sweeney (2009), would be needed, in addition to E-field transmission through the body and mapping of nerves and muscles in the human.

<sup>7</sup> The use of leg pull as the porcine measurement generally represents the case of using a measured surrogate response outside of the injury causal chain. Unless the measured response can, through surrogate system modeling, be mapped unambiguously to activity within the injury causal chain, only an empirical and difficult-to-generalize correlative transfer function remains.

- **Option 5: Voltage in body.** This construct would use the porcine data only to convert from applied voltage at the barbs to electrical potential within the body. This type of modeling may be available for the human body system, in which case the porcine system would be of little help. Modeling efforts include the Spatially Extended Nonlinear Node (SENN) model (Reilly and Diamant 2011), numerical simulation (Leitgeb et al. 2010), and efforts by AFRL to model electric field transmission through the pig, mouse and human body (Ibey 2014). It was outside the scope of this paper to evaluate fully all of these models. Nonetheless, no end-to-end model from voltage to risk of SCF is presently available.

Options 1 and 2, while offering a reduced burden on human biomechanical modeling, will unlikely lead to success because there is little similarity in muscle forces, geometry, and breaking forces of the vertebral bones in human and pigs.

Options 4 and 5 are also unlikely to be successful because the overall complexity of the end-to-end modeling of the human body response to EMI appears to be extremely high and, at the present time, most likely prohibitive for practical implementation.

The most feasible option to effectively use a porcine surrogate system appears to be Option 3 (Tendon forces). It requires sophisticated biomechanical models of the human body, which do exist. At the same time, it allows one to relate response of human muscles to the EMI doses via observation and measurement of porcine response, thereby eliminating the need for a prohibitively complex end-to-end human system response model. Human skeletal response to muscle activation might then be either tested through non-EMI stimulation or with the biomechanical model. Vertebrae injury criteria could be established with *in vitro* testing. In this case, the transfer function would correlate the pig-to-human muscle response to the EMI stimulus, and the biomechanical model would account for differences in muscle strength, perhaps timing due to nerve lengths, breaking vertebra bone strength, and so forth between humans and pigs.

Whether such a model and measurements would need to be dynamic and/or time resolved depends on the currently unknown considerations involved in the proximate cause of failure. The nerve impulse model would require measurement or inference of pig nerve impulses and a model for human muscle recruitment. Again, the necessity of dynamic and/or time-resolved measurements and models is currently unknown.



## 5. Conclusions and Roadmap

---

### A. Conclusions

Analysis of the differences between the human and pig spine and musculoskeletal system indicate that pigs are not a good surrogate for studying spinal loading and rate of compressive fracture in humans. The main difference can be summarized by the fact the pigs are quadrupeds, with significantly lower compressive strengths of the vertebrae.

The well-studied parameter space of various EMI waveforms does not include the exact conditions under which the AFRL researchers demonstrated a high rate of vertebral fracture in swine following EMI stimulus. Those conditions appear to be on the higher end of stimulus strength but, most importantly, were applied directly to the back, unlike most previous studies. This placement, along with seemingly small changes to the waveform parameters, resulted in a significantly different outcome, highlighting a need to understand better the effects of repetition rate, pulse charge, and duration on the contractile forces of muscles being stimulated locally. Existing data do not offer sufficient insights into the necessary relationships between waveform parameters and local muscle contraction to make predictions about the risk of SCF in either humans or swine going forward. However, based on a full review of the available data, we believe that experiments performed on the pig with dorsal application and typical TASER<sup>®</sup> parameters (or higher, as in the AFRL experiments) will continue to result in fracture and that EMI application to the human back with TASER<sup>®</sup> parameters will not. However, the tested parameter space of humans is much smaller than that of pigs, as seen in Figure 2-10.

An analysis of the human back musculoskeletal system reveals that humans are vulnerable to fracture due to forces induced by muscle contraction. The compressive forces induced by lifting heavy weights or performing everyday activities offer insights into the relative strength of human muscles vs. compressive strengths of the vertebrae. The key difference between such everyday activities (where vertebrae are infrequently fractured) and in conditions such as epilepsy, shock therapy, tetany, and EMI stimulus (where measured rates vary from less than 1% to 66%) is that the human body unconsciously optimizes (in time and space) the muscle response to such stresses in ways that distribute the forces and protect the vertebrae. Conditions such as epilepsy and tetany and external stimulus prevent the body from taking advantage of such measures.

With that in mind, we developed a generalized framework to assist in developing a roadmap for future study. The summary of our results using the framework are presented in the next section.

## **B. Road Map**

The most feasible option to use a porcine surrogate system effectively appears to be the development of a transfer function at the level of experimentation that measures tendon forces in the surrogate. This effort will require experimentation that provides time-and-space-resolved muscle contraction intensity as a function of distance from the probe, pulse repetition rate, pulse charge and duration, and use of existing finite element models of the human spine.

### **1. Surrogate Experimentation**

The experimental effort can be conducted in animal surrogates. Our analysis using the surrogate framework indicates that the pig will be a suitable surrogate for this level of experimentation. Experiments should be conducted to extend the existing knowledge base concerning the dependence of contractile force on distance from the probes and the waveform parameters of repetition rate, pulse charge, and duration.

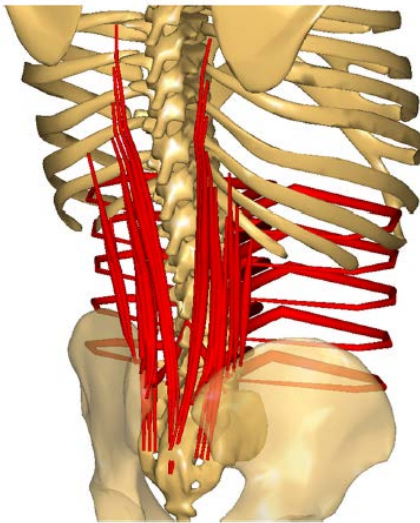
Multiple invasive and non-invasive experimental techniques to measure muscle contraction intensity have been developed. Some of these techniques have been used during electrical stimulation, indicating that interference of the EMI signal is a challenge that can be overcome experimentally. Such methods include electromyography (using deep or superficial needles), ultrasound imaging, magnetic resonance imaging, and acoustic myography. If possible, contours of constant maximum contractile force as a function of the parameters such as those generated in Figure 2-9 should be generated for different combinations of muscle groups and distances from the probes.

The result of this experimentation will be two-fold: (1) the JNLWD will have the ability to evaluate a proposed waveform in terms of contractile force dependence on waveform parameters, and (2) the inputs for a more in-depth computational evaluation of the human spine vulnerability to EMI-induced SCF will be provided.

### **2. Human Modeling**

In conjunction with such testing, sophisticated biomechanical models of the human body will be required to discover the conditions that cause fracture. Such models have been developed, although these models focus more on the lumbar region while the observed fractures in humans occurred in the thoracic region, (e.g., Granata and Marras 1993; Marras et al. 2001; Zander et al. 2015). After consultation with one of the authors, we believe that such models can be modified for the present effort (W. Marras (The Ohio State University), pers. comm., 2016). We recommend using such models first in reverse to identify the mechanism of fracture (i.e., what is the necessary combination of number of repetitions, contraction strength, time-induced asymmetric fatigue, or underlying pathology to create fracture?) and then with measured muscle contraction intensities to estimate actual rates of fracture.

The idea behind the inverse problem is to start with the critical level of stress in the vertebra and search for combinations of forces in the muscles around the spine that could lead to this stress (i.e., instead of solving for stresses in the vertebra for the given loading, solve for loading such that it would lead to fracture). We suggest that the current state of the art in human spine finite element analysis (FEA) models is sufficiently advanced to conduct such analysis. Figure 5-1 shows one such FEA model, which allows local geometry of tendons and forces to be analyzed. This model could be used to find what level of muscle tension (and in what muscles) may lead to critical vertebral stresses.



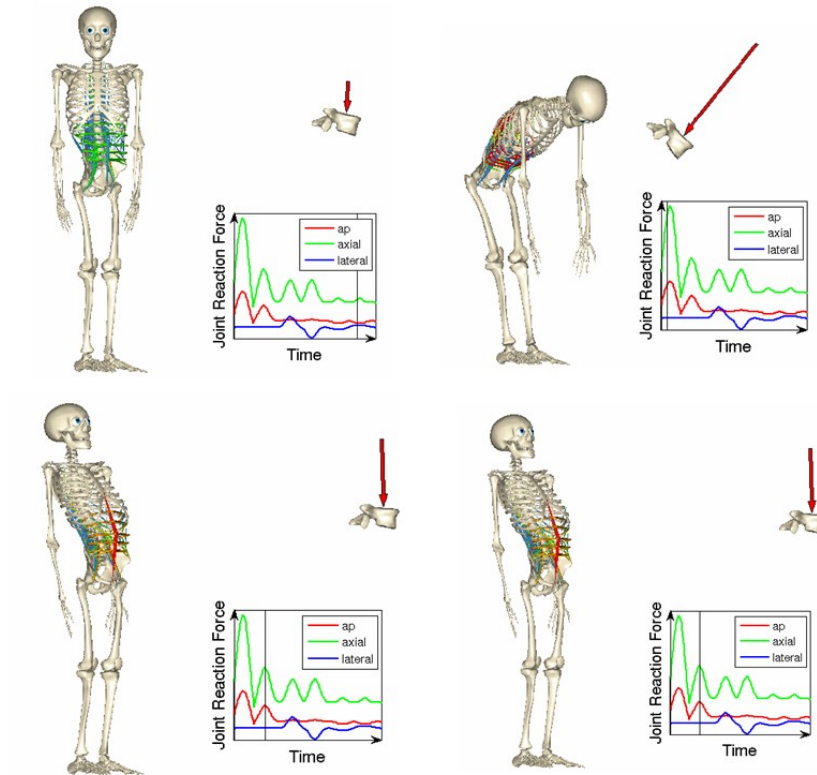
Source: Zander et al. (2015, 581).

**Figure 5-1. FEA Model of the Human Spine**

In addition, various body postures and motions can also have an effect on vertebral stress, and models have been developed to account for those postures and motions. Many FEA models use human bodies in motion, performing various activities, lifting weights, and so forth as an input to calculate loading forces on the bones and joints. Figure 5-2 shows one example of such models.

In this work, inverse dynamic models were used to estimate forces and moments acting on the spine and at surrounding structures from observed motions. These loads allow evaluation of the stress conditions in joints, joint cartilage, bone, muscles, tendons, and ligaments.

To conclude, we suggest that “discovering” which muscles, when fully recruited, generate forces sufficient to fracture vertebra (combined with the action of other forces or alone) would allow us to rule out waveforms that lead to a higher risk of injury and narrow the search and reduce the burden of optimizing the EMI waveform. Such work will be



Source: Julius Wolff Institute for Biomechanics and Musculoskeletal Regeneration (2016).

**Figure 5-2. Muscle Activities and Joint Reaction Forces at Lumbar Level L4/L5 during Flexion, Extension, Lateral Bending, and Axial Rotation**

essential for evaluating the RSI due to SCF. If this evaluation is the primary purpose of the effort, we recommend completing this computational experimentation before embarking on the characterization of the local time-and-space-resolved muscle effects of EMI since the results of modeling will inform the parameter space of interest for experimentation. If the JNLWD desires to understand the full parameter space of EMI weapons, experimentation and computational work can be done in parallel.

# Illustrations

---

## Figures

Figure 2-1. Set Up for the AFRL 2015 SCF Experiment .....	2-2
Figure 2-2. Muscle Tension as a Function of Stimulus Rate.....	2-4
Figure 2-3. Dependence of Net Force of a Suspended Swine Limb Attached to a Strain Gauge on EMI Waveform Parameters of Electrode Separation, Pulse Repetition Rate, and Charge Delivered per Pulse.....	2-6
Figure 2-4 Example Voltage and Current Waveform of a Commercial CEW Pulse (Top) and a Square Pulse from the Laboratory Device (Bottom).....	2-7
Figure 2-5. Simulated Contraction Forces as a Function of Stimulus Repetition Rate ...	2-9
Figure 2-6. Simulated Relative Force Normalized to TASER X26 Leg-Pull as a Function of Pulse Repetition Rate .....	2-10
Figure 2-7. Total Pulse charge vs Percent X26 Response .....	2-11
Figure 2-8. Extrapolated Bands of Normalized Force as a Function of Charge per Pulse.....	2-12
Figure 2-9. Normalized Force Contours (Based on Leg-Pull Data) .....	2-14
Figure 2-10. Parallel Coordinates Plot of Known, Experimentally or Field Tested Parameters in (a) Swine and (b) Humans .....	2-16
Figure 3-1. The Human Spine.....	3-2
Figure 3-2. The Human Spine: Deep Back Muscle Groups Relevant to Motion and Stability.....	3-2
Figure 3-3. Cross-Sectional View through T9 Highlighting the Topographic Organization of the erector Spinae and the Transversospinal Group of Muscles ..	3-3
Figure 3-4. Diagrammatic Representation of the Spatial Orientation of the Lines of Force of the Intrinsic Muscular Stabilizers.....	3-3
Figure 3-5. Ten Activities with the Highest Maximum Resultant Force.....	3-4
Figure 3-6. Forces on the Vertebral Bodies .....	3-5
Figure 3-7 Averaged Strength of Thoracic (T8-T10) and Lumbar (L3-L5) Strength for Women and Men of Various Ages.....	3-6
Figure 3-8. Correlation of Vertebral Failure Loads of T10 and L3 in Both Genders.....	3-7
Figure 3-9 EMG Responses (Intensity and Onset Time) during Arm Flexing.....	3-8
Figure 4-1. Surrogate Framework.....	4-1
Figure 4-2. Lumped Transfer Function Construct .....	4-2
Figure 4-3. Similarity/Modeling Complexity Tradeoff .....	4-4
Figure 4-4. Schematic Diagram of a General Pig-to-Human Transfer Function.....	4-6

Figure 4-5. Anatomical Dimensions Measured per Vertebra .....	4-7
Figure 4-6. Upper End-Plate Dimensions of the Human and Porcine Vertebra.....	4-8
Figure 5-1. FEA Model of the Human Spine.....	5-3
Figure 5-2. Muscle Activities and Joint Reaction Forces at Lumbar Level L4/L5 during Flexion, Extension, Lateral Bending, and Axial Rotation .....	5-4

**Table**

Table 2-1 The Intersection of the Waveform Parameters Used in the AFRL Study with the Maximum and Minimum Percentage of X26 Estimates Produced by IDA .....	2-12
---	------

## References

---

- Angelidis Matthew, Amaya Basta, Marilyn Walsh, H. Range Hutson, and Jared Strote. 2009. "Injuries Associated with Law Enforcement Use of Conducted Electrical Weapons." Supplement. *Academic Emergency Medicine* 16 (4) (April): S 229 (Abstract 569). <http://onlinelibrary.wiley.com/doi/10.1111/j.1553-2712.2009.00391.x/epdf>.
- Beason, Charles W., James R. Jauchem, C. D. Clark, III, James E. Parker, and David A. Fines. 2009. "Pulse Variations of a Conducted Energy Weapon (Similar to TASER® X26 Device): Effects on Muscle Contraction and Threshold for Ventricular Fibrillation." *Journal of Forensic Sciences* 54 (5) (September): 1113–1118. <http://onlinelibrary.wiley.com/doi/10.1111/j.1556-4029.2009.01129.x/epdf>.
- Bozeman, William P., William E. Hauda, II, Joseph J. Hecj, Derrel D Graham, Jr., Brian P. Martin, and James E. Winslow. 2009. "Safety and Injury Profile of Conducted Electrical Weapons Used by Law Enforcement Officers against Criminal Suspects." *Annals of Emergency Medicine* 53 (4) (April): 480–489. <http://dx.doi.org/10.1016/j.annemergmed.2008.11.021>.
- Brewer, James E., and Mark W. Kroll. 2009. "Field Statistics Overview." Chap. 24 in *TASER® Conducted Electrical Weapons: Physiology, Pathology, and Law*, edited by Mark W. Kroll and Jeffrey D. Ho. New York, NY: Springer-Kluwer.
- Bridwell, Keith. 2016a. "Facet Joints of the Spine's Anatomy." Last updated October 13. <https://www.spineuniverse.com/anatomy/facet-joints-spines-anatomy>.
- Bridwell, Keith. 2016b. "Vertebral Column." Last updated October 13. <https://www.spineuniverse.com/anatomy/vertebral-column>.
- Bürklein D., E.-M. Lochmüller, V. Kuhn, J. Grimm, R. Barkmann, R. Müller, and F. Eckstein. 2001. "Correlation of Thoracic and lumbar Vertebral Failure Loads with *In Situ* vs. *Ex Situ* Dual Energy X-ray Absorptiometry." *Journal of Biomechanics* 34 (5) (May): 579–587. [http://dx.doi.org/10.1016/S0021-9290\(01\)00010-0](http://dx.doi.org/10.1016/S0021-9290(01)00010-0).
- Burns, J., M. Kamykowski, J. Moreno, J., and M. Jirjis. 2015. "Prolonged Electro-muscular Incapacitation (EMI) in a Porcine Model for Assessment of Spinal Injury." San Antonio, TX: JBSA Fort Sam Houston, General Dynamics Information Technology.
- Busscher, Iris, Joris J. W. Ploegmakers, Gijsbertus J. Verkerke, and Albert G. Veldhuisen. 2010. "Comparative Anatomical Dimensions of the Complete Human and Porcine Spine." *European Spine Journal* 19 (7) (July): 1104–1114. [doi:10.1007/s00586-010-1326-9](https://doi.org/10.1007/s00586-010-1326-9).

- Cholewicki, J., S. M. McGill, and R. W. Norman. 1991. "Lumbar Spine Loads during the Lifting of Extremely Heavy Weights." *Medicine and Science in Sports and Exercise* 23 (10) (October): 1179–1186. [http://glaucoma.publicaciones.saludcastillayleon.es/acsm-msse/Abstract/1991/10000/Lumbar\\_spine\\_loads\\_during\\_the\\_lifting\\_of\\_extremely.12.aspx](http://glaucoma.publicaciones.saludcastillayleon.es/acsm-msse/Abstract/1991/10000/Lumbar_spine_loads_during_the_lifting_of_extremely.12.aspx).
- Comeaux, James A., James R. Jauchem, D. Duane Cox, Carrie C. Crane, and John A. D'Andrea. 2013. "40-Hz Square-Wave Stimulation Requires Less Energy to Produce Muscle Contraction: Compared with the TASER® X26 Conducted Energy Weapon." *Journal of Forensic Sciences* 58 (4) (July): 1026–1031. <http://onlinelibrary.wiley.com/doi/10.1111/1556-4029.12122/pdf>.
- Eastman, Alexander L., Jeffrey C. Metzger, Paul E. Pepe, Fernando L. Benitez, James Decker, Kathy J. Rinnert, Craig A. Field, and Randall S. Friese. 2008. "Conductive Electrical Devices: A Prospective, Population-Based Study of the Medical Safety of Law Enforcement Use." *The Journal of Trauma and Acute Care Surgery* 64 (6) (June): 1567–1572. <https://www.ncbi.nlm.nih.gov/pubmed/18545125>.
- Finelli, P. F., and J. K. Cardi. 1989. "Seizure as a Cause of Fracture." *Neurology* 39 (6) (June): 858–860. <https://www.ncbi.nlm.nih.gov/pubmed/2725885>.
- Granata, K. P., and W. S. Marras. 1993. "An EMG-Assisted Model of Loads on the Lumbar Spine during Asymmetric Trunk Extensions." *Journal of Biomechanics* 26 (12) (December): 1429–1438. <http://www.sciencedirect.com/science/article/pii/002192909390093T>
- Ho, Jeffrey D., Donald M. Dawes, and James R. Miner. 2009. "Serum Biomarker Effect of Prolonged TASER® XREP Device Exposure." Minneapolis, MN: Hennepin County Medical Center. [https://www.wired.com/images\\_blogs/dangerroom/2009/07/ho-serum-biomarker-xrep-1.pdf](https://www.wired.com/images_blogs/dangerroom/2009/07/ho-serum-biomarker-xrep-1.pdf).
- Ho, Jeffrey D., Donald M. Dawes, Laura L. Bultman, Jenny L. Thacker, Lisa D. Skinner, Jennifer M. Bahr, Mark A. Johnson, and James R. Miner. 2007. "Respiratory Effect of Prolonged Electrical Weapon Application on Human Volunteers." *Academic Emergency Medicine* 14 (3) (March): 197–201. <http://onlinelibrary.wiley.com/doi/10.1197/j.aem.2006.11.016/epdf>.
- Ho, Jeffrey D., Donald M. Dawes, Robert F. Reardon, Seth R. Strote, Sebastian N. Kunz, Rebecca S. Nelson, Erik J. Lundin, Benjamin S. Orzoco, and James R. Miner. 2011. "Human Cardiovascular Effects of a New Generation Conducted Electrical Weapon." *Forensic Science International* 204 (1–3) (January): 50–57. <http://www.sciencedirect.com/science/article/pii/S0379073810002343>.
- Home Office. 2011. "Figures on the Reported and Recorded Uses of Taser by Police Forces in England and Wales." Sandridge, St Albans, Hertfordshire: Home Office, March 21. [https://www.gov.uk/government/uploads/system/uploads/attachment\\_data/file/115676/taser-figures-march-2010.pdf](https://www.gov.uk/government/uploads/system/uploads/attachment_data/file/115676/taser-figures-march-2010.pdf).

- Hopkins, P., and K. Beary. 2003. *TASER Use and Officer/Suspect Injuries*. Orlando, Florida: Orange County Sheriff's Office. As cited in Mesloh, Charlie, Mark Henych, and Ross Wolf. 2008. *Less Lethal Weapon Effectiveness, Use of Force, and Suspect & Officer Injuries: A Five-Year Analysis*. Document No. 224081. Washington, DC: National Institute of Justice. <https://www.ncjrs.gov/pdffiles1/nij/grants/224081.pdf>.
- Ibey, Bennett L. 2014. "Nanosecond Electrical Pulse Bioeffects: Simulation of the Electric Field at the Spinal Cord in a Human Model." White Paper. JBSA Fort Sam Houston, TX: Air Force Research Laboratory, Radio Frequency Bioeffects Branch, Bioeffects Division, Human Effectiveness Directorate, 711<sup>th</sup> Human Performance Wing.
- Iyer, Sravisht, Blaine A. Christiansen, Benjamin J. Roberts, Michael J. Valentine, Rajaram K. Manoharan, and Mary L. Bouxsein. 2010. "A Biomechanical Model for Estimating Loads on Thoracic and Lumbar Vertebrae." *Clinical Biomechanics* 25 (9) (November): 853–858. <http://dx.doi.org/10.1016/j.clinbiomech.2010.06.010>.
- Jackson, Emma, Clare Neeson, and Anthony Bleetman. 2006. "The Relative Risk of Police Use-of-Force Options: Evaluating the Potential for Deployment of Electronic Weaponry." *Journal of Clinical Forensic Medicine* 13 (5) (July): 229–241. <http://dx.doi.org/10.1016/j.jcfm.2005.11.006>.
- Jauchem, James R., Ronald L. Seaman, and Curtis M. Klages. 2009. "Physiological Effects of the TASER<sup>®</sup> C2 Conducted Energy Weapon." *Forensic Science, Medicine, and Pathology* 5 (3) (September): 189–198. [doi:10.1007/s12024-009-9100-1](https://doi.org/10.1007/s12024-009-9100-1).
- Jauchem, James R. 2010. "Repeated or Long-Duration TASER<sup>®</sup> Electronic Control Device Exposures: Acidemia and Lack of Respiration," *Forensic Science, Medicine, Pathology* 6 (1) (March): 46–53. [doi:10.1007/s12024-009-9126-4](https://doi.org/10.1007/s12024-009-9126-4).
- Jauchem, James R. 2015. "Exposures to Conducted Electrical Weapons (Including TASER<sup>®</sup> Devices): How Many and for How Long Are Acceptable?" Supplement. *Journal of Forensic Sciences* 60 (s1): S116–S1129. [doi:10.1111/1556-4029.12672](https://doi.org/10.1111/1556-4029.12672).
- Jirjis, Michael. 2015. *HEMI Technical Report*. JBSA Fort Sam Houston, TX: Air Force Research Laboratory.
- Joint Non-Lethal Weapons Directorate. 2009. *Counter-Personnel Initial Capabilities Document*. Quantico VA: JNLWD.
- Julius Wolff Institute for Biomechanics and Musculoskeletal Regeneration. 2016. "Inverse Dynamic Models of the Spine." [https://jwi.charite.de/en/research/spine\\_biomechanics/spinal\\_loads/invers\\_dynamic\\_models/](https://jwi.charite.de/en/research/spine_biomechanics/spinal_loads/invers_dynamic_models/).
- Kelly, J. P. 1954. "Fractures Complicating Electro-Convulsive Therapy and Chronic Epilepsy". *Journal of Joint and Bone Surgery* 36B (1) (February): 70–79. <http://www.bjj.boneandjoint.org.uk/content/jbjsbr/36-B/1/70.full.pdf>.
- Kenny, J., C. Bass, W. Bozeman, V. Bovbjerg, D. Farrer, R. Ideker, and J. Mortimer. 2012. *The Human Effects Advisory Panel's Assessment of the HEMI RSI and Efficacy Study*. University Park, PA: Penn State University.

- Kroll, Mark W., Dorin Panescu, Matthew Carver, Ryan M. Kroll, and Andrew F. Hinz. 2009. "Cardiac Effects of Varying Pulse Charge and Polarity of TASER<sup>®</sup> Conducted Energy Weapons." *Proceedings of the 2009 Annual International Conference of the IEEE Engineering in Medicine and Biology Society* 2009: 3195–3198. doi:[10.1109/IEMBS.2009.5333135](https://doi.org/10.1109/IEMBS.2009.5333135).
- Leitgeb, N., F. Niedermayr, R. Neubauer, and G. Loos. 2010. "Numerically Simulated Cardiac Exposure to Electric Current Densities Induced by TASER X-26 Pulses in Adult Men." *Physics in Medicine and Biology* 55 (20) (September): 6187–6195. doi:[10.1088/0031-9155/55/20/010](https://doi.org/10.1088/0031-9155/55/20/010).
- Luttgens, Kathryn, and Nancy Hamilton. 1997. *Kinesiology: Scientific Basis of Human Motion*. 9<sup>th</sup> ed. Madison, WI: Brown & Benchmark.
- Mann, Michael D. 2016. *The Nervous System in Action*. Last updated 12/01/2011. <http://michaeldmann.net/The%20Nervous%20System%20In%20Action.html>.
- McDaniel, Wayne C., Robert A. Stratbucker, Max Nerheim, and James E. Brewer. 2005. "Cardiac Safety of Neuromuscular Incapacitating Defensive Devices." Supplement. *Pacing and Clinical Electrophysiology* 28 (Suppl. 1) (January): S284–S287. <https://www.ncbi.nlm.nih.gov/pubmed/15683517>.
- Marras, W. S., M. J. Jorgensen, K. P. Granata, and B. Wiand. 2001. "Female and Male Trunk Geometry: Size and Prediction of the Spine Loading Trunk Muscles Derived from MRI." *Clinical Biomechanics* 16 (1) (January): 38–46. [http://dx.doi.org/10.1016/S0268-0033\(00\)00046-2](http://dx.doi.org/10.1016/S0268-0033(00)00046-2).
- Mosekilde, Lis, Jakob Kragstrup, and Alan Richards. 1987. "Compressive Strength, Ash Weight, and Volume of Vertebral Trabecular Bone in Experimental Fluorosis in Pigs." *Calcified Tissue International* 40 (6) (June): 318–322. doi:[10.1007/BF02556693](https://doi.org/10.1007/BF02556693).
- Neumann, Donald A. 2010. *Kinesiology of the Musculoskeletal System: Foundations for Rehabilitation*. 2<sup>nd</sup> ed. Milwaukee, WI: Mosby.
- Pakhomov, Andrei, Juergen F. Kolb, Ravindra P. Joshi, Karl H. Schoebnach, Thomas Dayton, James Comeaux, John Ashmore, and Charles Beason. 2006. "Neuromuscular Disruption with Ultrashort Electrical Pulses." *Proceedings of SPIE* 6219 (May 26): 621903-1–621903-8. doi:[10.1117/12.665617](https://doi.org/10.1117/12.665617).
- Pig Manual*. n.d. <http://expedioscientiam.net/slhs/miscFiles/bio/pigManual.pdf>.
- Polga, David J., Brian P. Beaubien, Patricia M. Kallemeier, Kurt P. Schellhas, William D. Lew, Glenn R. Buttermann, and Kirkham B. Wood. 2004. "Measurement of *In Vivo* Intradiscal Pressure in Healthy Thoracic Intervertebral Discs." *Spine* 29 (12) (June): 1320–1324. <https://www.ncbi.nlm.nih.gov/pubmed/15187632>.
- Reilly, J. Patrick, and Alan M. Diamant. 2011. "Electric Stun Devices and Electric Shock." Chap. 10 in *Electrostimulation: Theory, Applications, and Computational Model*. Norwood, MA: Artech House.

- Rohlmann, Antonius, David Pohl, Alwina Bender, Friedmar Graichen, Jörn Dymke, Hendrik Schmidt, and Georg Bergmann. 2014. "Activities of Everyday Life with High Spinal Loads." *PLoS ONE* 9 (5) (May 27): e98510. <http://journals.plos.org/plosone/article/asset?id=10.1371/journal.pone.0098510.PDF>.
- Roy, O. Z., and A. S. Posgorski. 1989. "Test on a Shocking Device—The Stun Gun." *Medical & Biological Engineering and Computing* 27 (4) (July): 445–448. [https://www.researchgate.net/publication/20553691\\_Tests\\_on\\_a\\_shocking\\_device-The\\_stun\\_gun](https://www.researchgate.net/publication/20553691_Tests_on_a_shocking_device-The_stun_gun).
- Samelson, Elizabeth J., Blaine A. Christiansen, Serkalem Demissie, Kerry E. Broe, Qiong Louie-Gao, L. Adrienne Cupples, Benjamin J. Roberts, Rajaram Manoharam, John D'Agostino, Thomas Lang, et al. 2012. "QCT Measures of Bone Strength at the Thoracic and Lumbar Spine: The Framingham Study." *Journal of Bone and Mineral Research* 27 (3) (March): 664–663. doi:[10.1002/jbmr.1482](https://doi.org/10.1002/jbmr.1482).
- Sherman, Arthur J., James H. Luciano, and Dorothy S. Vander. 1970. *Human Physiology, the Mechanisms of Body Function*. New York, NY: McGraw-Hill Book Company.
- Sherry, Clifford, Carroll Brown, Charles Beason, Thomas Dayton, James Ross, James Jauchem, Leland Johnson, and Charles Kuhnel. 2003. *An Evaluation of the Electrical Properties and Bio-Behavioral Effects of Four Commercially Available Tasers and the JAYCOR Sticky Shocker*. Technical Report AFRL-HE-BR-TR-2003-0089. Brooks City-Base, TX: United States Air Force Research Laboratory, Human Effectiveness Directorate, Directed Energy Bioeffects Division, Radio Frequency Radiation Branch, June. <http://www.dtic.mil/dtic/tr/fulltext/u2/a416553.pdf>.
- Sloane, Christian M., Theodore C. Chan, and Gary M. Vilke. 2008. "Thoracic Spine Compression Fracture after TASER Activation." *Journal of Emergency Medicine* 34 (3) (April): 283–285. <http://dx.doi.org/10.1016/j.jemermed.2007.06.034>.
- Sweeney, James D. 2009. "Theoretical Comparisons of Nerve and Muscle Activation by Neuromuscular Incapacitation Devices." *Proceedings of the IEEE Engineering in Medicine and Biology Society* 2009: 3188–3190. <https://www.ncbi.nlm.nih.gov/pubmed/19964799>.
- TASER Corporation Website. n.d. <https://www.taser.com/>.
- TASER. n.d. "TASER X26P." Accessed October 26, 2016. <https://www.taser.com/products/x26p>.
- Urquhart, Donna M., Paul W. Hodges, and Ian H. Story. 2005. "Postural Activity of the Abdominal Muscles Varies between Regions of These Muscles and between Body Positions." *Gait and Posture* 22 (4) (December): 295–301. <http://dx.doi.org/10.1016/j.gaitpost.2004.09.012>.
- Valentino, Daniel J., Robert J. Walter, Andrew J. Dennis, Kimberly Nagy, Michele M. Loor, Jerry Winners, Faran Bokhari, Dorion Wiley, Asher Merchant, Kimberly Joseph, and Roxanne Roberts. 2007. "Neuromuscular Effects of Stun Device Charges." *Journal of Surgical Research* 143 (1) (November): 78–87. <http://dx.doi.org/10.1016/j.jss.2007.03.049>.

- Vasconcelos, Daniel. 1973. "Compression Fractures of the Vertebrae during Major Epileptic Seizures." *Epilepsia* 14 (3) (September): 323–328. <http://onlinelibrary.wiley.com/doi/10.1111/j.1528-1157.1973.tb03967.x/pdf>.
- Werner, Jacob R., David M. Jenkins, W. Bosseau Murray, Edward L. Hughes, David A. Bienus, and Mary J. Kennett. 2012. "Human Electromuscular Incapacitation Devices Characterization: A Comparative Study on Stress and the Physiological Effects on Swine." *Journal of Strength Conditioning and Research* 26 (3) (March): 804–810. <https://www.ncbi.nlm.nih.gov/pubmed/22173626>.
- Winslow, James E., William P. Bozeman, Michael C. Fortner, and Roy L. Alson. 2007. "Thoracic Compression Fractures as a Result of Shock from a Conducted Energy Weapon: A Case Report." *Annals of Emergency Medicine* 50 (5) (November): 584–586. <http://dx.doi.org/10.1016/j.annemergmed.2007.06.008>.
- Zander, Thomas, Marcel Dreischarf, Hendrik Schmidt, Georg Bergmann, and Antonius Rohlmann. 2015. "Spinal Loads as Influenced by External Loads: A Combined *In Vivo* and *In Silico* Investigation." *Journal of Biomechanics* 48 (4) (February 26): 578–584. <http://dx.doi.org/10.1016/j.jbiomech.2015.01.011>.

## Abbreviations

---

AFRL	Air Force Research Laboratory
CEW	Conducted Energy Weapon
EMG	electromyographic
EMI	Electromuscular Incapacitation
IDA	Institute for Defense Analyses
FEA	finite element analysis
IEEE	Institute of Electrical and Electronics Engineers
JBSA	Joint Base San Antonio
JNLWD	Joint Non-Lethal Weapons Directorate
MRG	McIntyre, Richardson, and Grill
NAMRU	Naval Medical Research Unit
pps	pulses per second
RSI	risk of significant injury
SCF	spinal compression fracture
SENN	Spatially Extended Nonlinear Node
SWaP	size, weight, and power
UEPD	Upper End Plate Depth
UEPW	Upper End Plate Width
VBR	vertebral body replacement



**REPORT DOCUMENTATION PAGE***Form Approved*  
OMB No. 0704-0188

The public reporting burden for this collection of information is estimated to average 1 hour per response, including the time for reviewing instructions, searching existing data sources, gathering and maintaining the data needed, and completing and reviewing the collection of information. Send comments regarding this burden estimate or any other aspect of this collection of information, including suggestions for reducing the burden, to Department of Defense, Washington Headquarters Services, Directorate for Information Operations and Reports (0704-0188), 1215 Jefferson Davis Highway, Suite 1204, Arlington, VA 22202-4302. Respondents should be aware that notwithstanding any other provision of law, no person shall be subject to any penalty for failing to comply with a collection of information if it does not display a currently valid OMB control number.

**PLEASE DO NOT RETURN YOUR FORM TO THE ABOVE ADDRESS.**

1. REPORT DATE November 2016		2. REPORT TYPE Final		3. DATES COVERED (From-To) Sep 2016 – Nov 2016	
4. TITLE AND SUBTITLE  Roadmap to Evaluate the Risk of Spinal Compression Fracture (SCF) Due to Electromuscular Incapacitation (EMI)				5a. CONTRACT NUMBER HQ0034-14-D-0001	
				5b. GRANT NUMBER	
				5c. PROGRAM ELEMENT NUMBER	
6. AUTHOR(S)  Kramer, Corinne M. Teichman, Jeremy A. Macheret, Yevgeny				5d. PROJECT NUMBER DU-2-4140	
				5e. TASK NUMBER	
				5f. WORK UNIT NUMBER	
7. PERFORMING ORGANIZATION NAME(S) AND ADDRESS(ES)  Institute for Defense Analyses 4850 Mark Center Drive Alexandria, VA 22311-1882				8. PERFORMING ORGANIZATION REPORT NUMBER  IDA Document D-8268	
9. SPONSORING / MONITORING AGENCY NAME(S) AND ADDRESS(ES)  Joint Non-Lethal Weapons Directorate 3097 Range Road Quantico, VA 22134-5100				10. SPONSOR/MONITOR'S ACRONYM(S)  JNLWD	
				11. SPONSOR/MONITOR'S REPORT NUMBER(S)	
12. DISTRIBUTION/AVAILABILITY STATEMENT  Approved for public release; distribution is unlimited (21 February 2017).					
13. SUPPLEMENTARY NOTES					
14. ABSTRACT Recent swine testing of a new Electromuscular Incapacitation (EMI) waveform performed at the Air Force Research Laboratory (AFRL) in 2012 produced spinal compression fracture (SCF) in the test subjects and was subsequently confirmed by another experiment in 2015. With a dorsal application of the new EMI stimulus, 43% of all swine subjects experienced a fracture (confirmed by necropsy). Such reports had never been documented in swine (even under similar conditions and waveform parameters, although probe placement varied). Such fractures in humans as a result of EMI use have been reported only twice in the literature. The lack of such reports in humans establishes as negligible the risk of significant injury (RSI) of SCF in the human population using currently fielded weapons. Overall risk of fracture injuries (to include those caused by falls) has been estimated at less than 0.5%. As efforts go forward to improve the EMI weapon for military use, changes may be made to the waveform that could alter the acceptable rate of SCF to humans. Given the inability to conduct human testing of new waveforms, the risk cannot be tested directly. The purpose of this document is to develop a roadmap for the evaluation of risk of significant SCF to humans in light of the new information provided by the AFRL experiment.					
15. SUBJECT TERMS Human Electromuscular Incapacitation (HEMI); human injury modeling; Non-lethal; spinal; compression fracture; surrogate framework; surrogate testing; TASER; vertebral fracture					
16. SECURITY CLASSIFICATION OF:			17. LIMITATION OF ABSTRACT	18. NUMBER OF PAGES	19a. NAME OF RESPONSIBLE PERSON
a. REPORT Uncl.	b. ABSTRACT Uncl.	c. THIS PAGE Uncl.			Dr. Shannon Foley
			SAR	57	19b. TELEPHONE NUMBER (include area code) 703-432-0900